Genetically encodable calcium sensors for Magnetic Resonance Imaging

by
Souparno Ghosh

B.Tech. (Hons.), Biotechnology and Biochemical Engineering
Indian Institute of Technology, Kharagpur, 2011

Submitted to the Department of Biological Engineering
in partial fulfillment of the requirements for the degree of

Doctor of Philosophy in Biological Engineering
at the
Massachusetts Institute of Technology

September 2018

Signature of Author: Signature redacted
Department of Biological Engineering
August 22, 2018

Certified by: Signature redacted
Alan Jasanoff
Professor of Biological Engineering,
Brain and Cognitive Sciences, Nuclear Science and Engineering
Thesis Supervisor

Accepted by: Signature redacted
Forest White
Professor of Biological Engineering,
Chair, Graduate Program Committee

Thesis Committee

Accepted by:_____ K. Dane Wittrup
Professor of Biological Engineering and Chemical Engineering
Chairman of Thesis Committee

Accepted by:_____ Alan Jasanoff
Professor of Biological Engineering, Brain and Cognitive Sciences,
and Nuclear Science and Engineering
Thesis Supervisor

Accepted by:_____ Jacquin C. Niles
Associate Professor of Biological Engineering
Thesis Committee Member

Genetically encodable calcium sensors for Magnetic Resonance Imaging

by
Souparno Ghosh

Submitted to the Department of Biological Engineering
on August 22, 2018 in partial fulfillment of
the requirements for the degree of Doctor of Philosophy
in Biological Engineering

ABSTRACT

A key requirement for understanding the workings of the brain is to fill in the explanatory gap between molecular phenomena and identifiable behavior at the organismal level. Magnetic resonance imaging (MRI) provides a unique tool for bridging this gap, as it allows for imaging tissue throughout whole organisms. Although functional MRI (fMRI) is already a workhorse technique in human neuroscience research, current fMRI methods give us limited information about brain mechanisms because they rely on blood flow changes that are only indirectly coupled to cellular and molecular events. To associate cellular or molecular specificity to MRI, there is a need for genetically targeted, analyte-specific sensors. Calcium is a molecule of great interest to biology since its fluctuations are highly correlated with neural activity. While much progress has been made in pursuit of genetically encoded calcium sensors none allow for deep tissue imaging of whole rodent brains.

In this thesis we demonstrate that genetically encodable calcium sensors based on known MRI gene reporter ferritin show modest sensitivity. To achieve higher amplification we leverage the hemodynamic response, which is coupled to neuronal activity through a calcium-activated enzyme, neuronal nitric oxide synthase (nNOS). We show that chemical stimulation of ectopically expressed neuronal nitric oxide synthase (nNOS) elicits an artificial hemodynamic response detectable by MRI. To distinguish signaling from endogenous nNOS we use a two-prong strategy to engineer a suite of enzymes with altered inhibition constants compared to nNOS. We demonstrate that these engineered enzymes (NOSTICs) exhibit calcium-dependent catalytic activity. One such NOSTIC was then virally delivered to rodent brains and shown to express in certain cell populations. Hemodynamic responses from these cell populations were recorded following electrical stimulation using MRI. The imaging strategy demonstrated here thus offers a novel and potentially powerful approach for cell-targeted functional imaging of the brain.

Thesis Supervisor: Alan Jasanoff
Title: Professor of Biological Engineering

ACKNOWLEDGMENTS

First and foremost I would like to express my heartfelt gratitude for Prof. Alan Jasanoff for giving me this amazing opportunity to learn, explore, and embrace taking on challenging problems. Alan has created a very unique lab atmosphere with a diverse set of expertise, approaching problems from different angles that facilitated my learning greatly. Alan has supported me both financially and intellectually, helping keep my eyes on the big picture while I was mired in troubleshooting.

I would also like to thank my committee members Prof. Wittrup and Prof. Niles. They have been supportive of some of the bold approaches I embarked on while at the same time highlighting potential pitfalls and ways I could solve them.

I have a number of colleagues to thank who have played an important role it this journey. Dr. Victor S. Lelyveld was instrumental in helping me acclimate with tissue culture practices and generous in sharing his expertise in protein biochemistry. Dr. Nan Li carried out a number of *in vivo* experiments, which are technically very challenging and rigorous. Dr. Benjamin B. Bartelle has been a collaborator and mentor extraordinaire as I have bounced numerous ideas off him as well sought his expertise when stuck troubleshooting.

For collaborations, strategizing, and discussions, I thank Dr. Ali Barandov, Dr. Peter Harvey, Dr. Yuri Matsumoto, Dr. Vivian Hsieh, Dr. Adrian L. Slusarczyk, and Jacob C. Simon. Thank you also to other members of the lab who have throughout the years been great colleagues.

Over the past seven years, I had the privilege of mentoring three outstanding undergraduate students --- Urvashi Singh, Sierra B. Weingartner, and Jade I. Daher. Having a front-row seat to their learning, development, and accomplishments have been one of the most rewarding experiences.

I would be remiss if I did not mention my fellow classmates from BE-2011. I have cherished their friendship and support. I have also found the biological engineering community at MIT to be very welcoming, accepting, and nourishing.

I thank Howard Hughes Medical Institute (HHMI) and the McGovern Institute of Brain Research at MIT for supporting me with fellowships.

Last but not the least, I would like to thank my parents whose unconditional love and support has been a constant. I am eternally grateful for the sacrifices they have made to give me the best opportunities in life, in particular the best education I could have.

TABLE OF CONTENTS

INTRODUCTION

One of the most enigmatic challenges for scientists is understanding, modeling, and ultimately reverse engineering the brain. The brain is a complex organ consisting of approximately 100 billion neurons [1] with an average of 7000 connections [2] to other neurons. Then there is the supporting cast of glial networks comprising of astrocytes, microglia, oligodendrocytes, and their progenitors NG2-glia [3]. There are phenomena that occur within milliseconds (e.g. neuronal firing) and others that take days to weeks (e.g. gene expression), all of which are critical to the functioning of the brain. There are structures ranging from as tiny as a dendritic spine (~ 0.1 μm^3) [4] to neuronal connections that span over millimeters that could hold the key towards our understanding of certain brain functions. Concentrations of essential chemical messengers (e.g. Ca2+) often fluctuate within 4 orders of magnitude [5] based on function and location thereby making their detection increasingly challenging. Finally, there is a network of epithelial cells lining the blood vessels that form a highly selective blood-brain barrier (BBB) that makes it extremely challenging to deliver exogenous agents to the brain. Expanding insight into the brain requires overcoming of a wide variety of challenges, but a key first step appears to be imaging.

1. IMAGING MODALITITES

Multiple imaging modalities help solve different parts of the puzzle. Electrophysiology is one such classical technique that allows us to precisely gauge the temporal responses of neurons to various stimuli [7]. It provides insight into the nature of responses (excitatory or inhibitory) and how responses are linked to different ion

channels [8, 9]. Electrical recordings have been made possible in awake rodents [10] and allows for recording from multiple cells types. Automation of patch clamping where robots have been programmed to detect cells seeks to the make the process for locating cells simpler [11]. Despite the precise nature of the information one can obtain from electrophysiology, it requires implantation of electrodes and is invasive. Its field of view is also extremely limited.

Optical microscopy allows for imaging at sub-cellular cellular resolution. Discovery and subsequent engineering of fluorescent proteins or genetically encodable optical reporters have resulted in their widespread use in optical microscopy [12, 13, 14, 15]. By harnessing the benefits of transgenic mouse lines combined with multiple fluorescent proteins, Livet and colleagues [16] used fluorescence microscopy to visualize multiple cell types *ex vivo*. Optical microscopy suffers from high background fluorescence that reduces image contrast. The advent of two-photon microscopy [17] allows for imaging of live tissue up to 1 mm in depth. In this technique, two near-infrared photons are used to excite a fluorophore that emits in the visible range. The use of longer wavelength near-infrared photons allows for greater tissue penetration depth, lower autofluorescence, less scatter, and a tight focal spot, although near-simultaneous excitation with two photons demands use of high-powered lasers.

While fluorescent proteins are excellent reporters, efforts to measure neural activity received a boost from a slew of genetically encodable calcium sensors [18, 19]. Striman and colleagues [20] combined two-photon microscopy with a genetically encodable calcium sensor and demonstrated the ability to visualize cortical neurons in

mice over an area > 9 mm^2. Despite these advances optical imaging remains limited in field of view with its depth limited to ~ 1 mm due to scattering by tissue.

Positron emission tomography (PET) is an alternative imaging technique that allows for whole-brain imaging *in vivo* [21, 22]. It generally involves using a radiolabeled metabolite-analogue that is injected into the blood stream. It can be used to determine metabolic rates in different regions of the brain. Though it requires only a small amount of tracer, is non-invasive, and provides whole brain coverage, these advantages are offset by poor spatial resolution, the required use of a radioactive molecule, and provide limited information about cell-types.

2. MAGNETIC RESONANCE IMAGING

Magnetic resonance imaging (MRI) provides a unique opportunity to image the whole brain in live animals with sub-second temporal resolution and < 1 mm spatial resolution [23]. Functional MRI (fMRI) has been used to image brain activity both in clinical settings as well as in studies in humans, primates, and rodents [24, 25, 26, 27]. fMRI, also referred to as blood oxygen-level dependent (BOLD) MRI measures changes in blood flow and volume and relies on hemoglobin present in blood to generate contrast [28, 29, 30]. While this technique precludes the need for addition of exogenous contrast agents and subsequent problems associated with their delivery to the brain, it provides limited information in terms of cell-types or cell-circuits. Its spatial resolution is limited by the arrangement of capillaries in the brain [31]. The magnitude of signal changes observed during an fMRI experiment can be often small requiring multiple acquisitions

and statistical analyses to determine signal from noise. Thus, despite the distinct benefits of being a non-invasive technique capable of whole-brain imaging of live animals there is ample scope for improvement especially with respect to cell-specificity and sensitivity.

The major area of improvement that this thesis aims to address is the development of genetically encodable molecular sensors for fMRI. Before discussing efforts to engineer MRI contrast agents, here is a brief discussion of alternative methods to look at other ways to improve upon the fMRI technology. In the pursuit of high-resolution images there is always a trade off with acquisition time. One could approach the theoretical limit of spatial resolution using MRI in the 1-10 μm range by using scan times greater than 1 hour [32, 33]. Yu and colleagues demonstrated that fMRI could be used to detect single venules and arterioles in rats on a 14T scanner with voxel sizes of 100 x 100 x 500 μm [34]. The same group, in another study, used a line scanning technique to achieve a 50 ms temporal resolution using a 11.7T scanner with voxel size of 50 μm x 1 mm x 1 mm [35]. One strategy deployed to reduce acquisition time is similar to one used in compression of JPEG images. This is known as *compressed sensing* where image reconstruction is based on fewer data points acquired [36]. Alternatively, to increase data points acquired in a given time scale, multi-coil systems can be employed [37]. Finally, ultra-high field imaging at higher than 20T is likely to be increasingly accessible [38]. Thus a combination of pulse sequences, multi-coil systems, high-filed scanners, and improved algorithms for image reconstructions can all contribute to improved sensitivity of fMRI applications.

3. MRI CONTRAST AGENTS

Contrast in MRI is achieved due to differential distribution of nuclear spins of a particular element (often water protons) present in the sample [39]. In the classical description of a nuclear magnetic resonance experiment, a strong constant magnetic field is applied, such that unpaired nuclear spins align with a net moment in the direction of the applied field. Following the application of a resonant radio frequency pulse at the proton precessional frequency, which rotates the net spin moment away from the applied static field, the moment is allowed to recover to its equilibrium orientation. This process is known as relaxation and is characterized by two components. Initially there is loss of transverse phase coherence among the spins that leads to a darkening signal followed by recovery of the magnetic moment in the longitudinal direction that gives a brightening signal. Molecules that have the ability to interact with nuclear spins or produce local magnetic field inhomogeneities can alter the relaxation rates and are known as contrast agents. The time taken by the spins to recover to their original orientation is different in the vicinity of these molecules than in rest of the sample, leading to brightening or darkening in MRI scans. The time taken for the loss of transverse phase coherence is denoted by T_2 and the time required for the recovery of the net magnetic moment in the longitudinal direction is denoted by T_1. The inverse of these relaxation times are relaxation rates, R_2 and R_1. Contrast agents are characterized by their ability to influence these relaxation rates in terms of concentration of agent, defined as their relaxivity (r_1/r_2, generally in units of $mM^{-1}s^{-1}$).

3.A. METALLIC COMPLEXES

Metal complexes with paramagnetic ions (with a partially filled d or f orbitals) form a family of contrast agents generally characterized by their effect on longitudinal relaxation rates [39]. One of the first contrast agents characterized and tested in rats was gadolinium diethylenetriaminepenta-acetic acid (Gd-DTPA) in 1983 [40]. Carr and colleagues used a 0.1 mmol/kg dose of Gd-DTPA to visualize brain tumors in human patients a year later [41]. In 1988, the US Food and Drug Administration (FDA) approved Gd-DTPA (Magnevist) for use in the central nervous system. There have since been ten other complexes approved by the FDA [42]. While there have been reports of metal accumulation in some patients treated with Gd-based contrast agents, more thermodynamically stable macrocyclic Gd-complexes appear to be a solution to that issue [43, 44].

Manganese-based complexes are another family of T_1 contrast agents that offer an alternative to Gd-complexes [45]. Troughtom and colleagues reported the synthesis of an Mn-EDTA complex with a diphenylcyclohexyl moiety for albumin binding [46]. The authors measured a nearly 10-fold increase in r_1 in presence of sera as compared to buffer without sera. Barandov *et al* synthesized a suite of Mn(III)-complexes based on the 1,2-phenylenediamine (PDA) ligand [47]. Esterified versions of these complexes were shown to accumulate intracellularly and following ester cleavage by endogenous esterases, provided a possibility for labeling cells with substrate-specific esterases. Manganese dipyridoxyl-diphosphate (Mn-DPDP) is an FDA injectable contrast agent approved for clinical use [48]. While Mn-based complexes continue to be avenue for improved contrast agents, Mn has also been used in MRI studies as $MnCl_2$ injections. Mn(II) is a

divalent cation that is capable of accumulation in neurons after entering through voltage-gated ion channels. Lin and Koretsky demonstrated the principle of manganese enhanced magnetic resonance imaging (MEMRI) [49]. The authors observed shortening of T_1 following continuous infusion of $MnCl_2$ in saline at 36 μmol/min. in anaesthetized rats. They stimulated the rats with glutamate in combination with BBB disruption and observed stimulation-dependent signal changes on the order of 200%. This application of MEMRI could be considered the first demonstration of functional imaging that was not dependent on blood flow. Further details of delivery of Mn in absence/presence of BBB disruption, kinetics, toxicity can be found in this review [50].

3.B. NANOPARTICLES

Super paramagnetic iron oxide nanoparticles (SPIOs) form the basis of another class of contrast agents. These SPIOs have a defined core size and cause shortening of T_2. SPIOs are generally coated with lipids, proteins, or nucleotides to make them biocompatible. Perez and colleagues demonstrated the ability of iron-oxide nanoparticles to sense a variety of bimolecular interactions *in vitro* [51]. Atanasijevic *et al* functionalized a set of SPIOs with calcium-binding protein calmodulin (CaM) and another set with CaM-binding peptide M13 or RS20. The authors demonstrated a clustering of these sets of nanoparticles in presence of titrated calcium, with the clustered complex displaying a five-fold higher relaxivity (r_2) compared to the two the sets of SPIOs alone. This was a demonstration of an MRI-readable, nanoparticle-based calcium sensor capable of detecting calcium fluctuations of ~1 μM *in vitro* [52]. Okada and colleagues further engineered magnetic calcium-responsive nanoparticles (MaCaReNas)

that were capable of sensing calcium fluctuations around 0.5 mM with a response time on the order of seconds [53]. The authors intracranially injected MaCaReNas in rat brains and observed signal changes in MRI in response to both chemical and electrophysiological stimuli. This was the first demonstration of molecular fMRI sensing calcium directly *in vivo*.

While both nanoparticle-based contrast agents and small molecule metal complexes can addresses the sensitivity problem (signal change in MRI per amount of contrast agent), there are significant barriers to delivering these agents to the brain. Additionally, while sensors like MaCaReNas can detect extracellular calcium fluctuations, intracellular calcium remains a prized target. There is also the need for genetic targeting of cell types or circuits with contrast agents that those discussed thus far do not achieve.

3.C. GENETICALLY ENCODED MRI REPORTERS

While MRI contrast agents have been designed to detect enzymatic activity [54, 55], one of the first demonstrations of a genetically encoded MRI reporter was made by Genove and colleagues [56]. The authors used a multimeric iron-sequestering protein ferritin as a contrast agent. A549 cells transduced with Adenovirus encoding for ferritin (Adv-Ft) and supplemented with ferric ammonium citrate (FAC) showed significantly higher contrast than A549 cells supplemented with FAC only. Interestingly the authors demonstrated that mice brains transduced with Adv-Ft produced a higher contrast enhancement compared to Adv encoding for the control Lac-Z gene in absence of any iron supplementation. In the same year, Cohen *et al* generated an engineered C6-glioma cell line that expressed ferritin and green fluorescence protein (GFP) [57]. These cells

were implanted in CD-1 nude mice and tumor formation could be visualized by ferritin-dependent contrast enhanced MRI. Since these reports, there have been efforts made to engineer ferritins to improve iron content and/or relaxivity. Iordanova and colleagues reported a chimeric protein constituting a fusion of light chain and heavy chain ferritin (L*H) that when transduced in U2OS cells had a 1.5 times higher R_2 than either of the ferritin subunits alone [58]. The same group, in a subsequent work demonstrated that the human mitochondrial ferritin without its mitochondrial localization sequence (cytoMTFT), when transduced in U2OS cells had caused moderate increase in iron-per-cell content compared to L*H [59]. Matsumoto and colleagues used a directed evolution strategy to enhance iron-loading capacity of ferritin derived from the thermophilic archaea *Pyrococcus furiosus* [60]. The engineered ferritin expressed in yeast yielded a 100% increase in R_2 compared to the wild type.

Despite the engineering efforts, conclusive evidence of ferritin as a MRI-readable genetic reporter for *in vivo* studies appears elusive [61]. MagA, an iron transporter from magnetotactic bacteria and DMT1, a divalent metal transporter (DMT1) were both used in separated studies as genetic MRI reporters [62, 63]. The bottleneck with employing metalloproteins or metal transporters as MRI reporters is that they typically require the supplementation of their cognate ions to see sufficient contrast. Supplementing these metals alone could confer some contrast enhancement, and depending on the nature of ion metabolism it is difficult to control the flux of these metals in cells.

Genetic reporters that do not rely on metal transport or metabolism have also been posited as potential MRI reporters. Human embryonic kidney (HEK) cells engineered to stably express urea transporter (UT-B) showed increased apparent water exchange rate

compared to controls [64]. Another study reported that aquaporin-expressing Chinese hamster ovary (CHO) cell xenografts that could be visualized in mice using diffusion weighted MRI [65].

In the examples of genetically encodable MRI agents discussed thus far, the target protein or the contrast agent was delivered either virally or via xenografts. There are examples of contrast agents that are purified proteins that can be delivered to rodent brains via intracranial injections. Shapiro and colleagues used a large scale screening method to improve the binding affinity of the flavocytochrome P450-BM3 for dopamine by more than 2 orders of magnitude [66]. A variant of that engineered protein was then used to map brain activation patterns in a rodent in response to electrical stimulation. This study was unique in that the activation pattern mapped was based on the prevalence of dopamine rather than hemodynamic response [67]. In an analogous study Hai *et al.* used another variant of the P450-BM3 protein that had been engineered for serotonin binding (K_d = 0.7 μM) to map serotonin reuptake in rats [68, 69]. By utilizing a molecular fMRI sensor the authors were able to measure serotonin transport dynamics in response to pharmacological perturbation across a large area of the brain.

It is clear that MRI provides unique capabilities as a tool for neuroscience through whole brain imaging of live animals. This chapter surveys efforts that have been made to gain more meaningful insight using MRI. One of the goals is to be able to associate MRI signals with circuits or specific cell types. Genetically encoded MRI reporters are prime targets. The icing on the cake would be genetically encodable MRI sensors i.e. molecules that could report on functional activity of neural or glial networks. This thesis details attempts to engineer genetically encodable, MRI-readable molecular sensors.

HEMOGENETIC IMAGING

1. ABSTRACT

Functional magnetic resonance imaging (fMRI) allows us to map brain activity across the entire brain with sub-second temporal resolution and < 100 μm spatial resolution. The activity maps are in reality a measure of localized changes in blood flow and volume. The signal changes observed could be a result of increased metabolic demand or due to activity from a mixture of neurons and glial cells. Thus, while it is possible to map out of physical locations in the brain that maybe active simultaneously, it is not possible to assign such activity patterns to a specific set of cells or a circuit. On the other hand advancements in genetic engineering have led to the generation of viral vectors that have been used to label cell populations in the brain. Here, we will demonstrate that by combining genetic targeting with the whole brain coverage of MRI, we can begin to identify cell populations responsible for observed fMRI patterns observed using a new technique we refer to as hemogenetic imaging.

2. INTRODUCTION

The mechanisms of neurovascular coupling (the connection between neuronal activity and hemodynamic response) have been intensely investigated. One suggested mechanism posits that glutamate activates N-methyl-D-aspartate (NMDA) receptors in excitatory neurons that then triggers increase in intra-cellular calcium concentrations. Ca^{2+} activates the neuronal nitric oxide synthase (nNOS) enzyme that catalyzes the formation of nitric oxide (NO) and L-citrulline from L-arginine. NO is a freely diffusing

gas that activates smooth muscle cells which in turn leads to vasodilation [70]. Calcium also activates phospholipase A that catalyzes the formation of arachidonic acid, which leads to subsequent synthesis of vasoactive prostaglandins [71]. Studies with nNOS knockout mice reveal that stimulation dependent changes in blood flow are affected to varying degrees in mice lacking nNOS depending on the location of the brain where blood flow is being measured [72, 73]. However, pharmacological inhibition of NOS affects blood flow and abrogates ~60% of BOLD signal induced by somatosensory stimuli [74, 75]. Thus, nNOS emerges as a potential genetically encodable target that links neuronal activity to hemodynamic response. In essence if specific cell types were labeled with nNOS one could probe the activity of those selected cells under a certain experimental paradigm provided there was a way to distinguish signaling from those cells and signaling from endogenous nNOS.

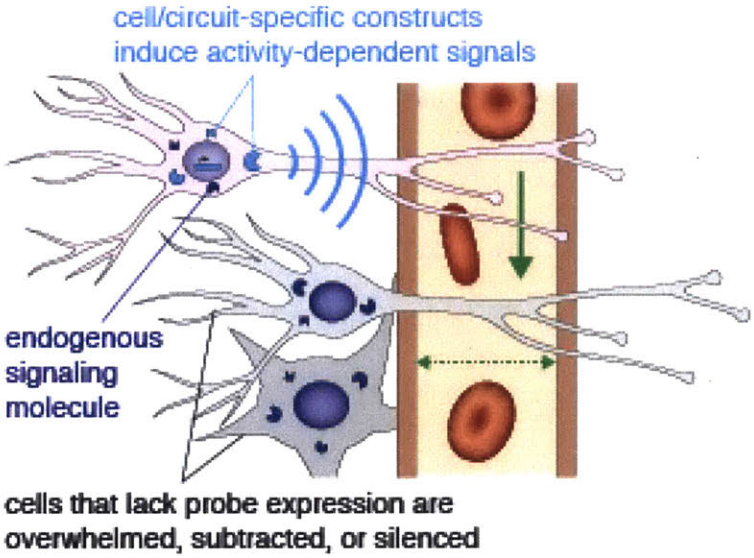

Fig 1. In this figure there are cells with nNOS (dark blue), an endogenous signaling molecule and cells with both nNOS and NOSTIC (light blue), a cell-specific construct that induces an artificial hemodynamic response when activated. In presence of nNOS-specific inhibitor signal from endogenous NOS is absent while NOSTIC is still active. This strategy outlines how signaling from an MRI experiment can be assigned to certain cell types.

Here, we engineered NOS and expressed them in specific cell types in order to eventually be able to trigger an artificial hemodynamic response. The idea of hijacking the hemodynamic response using vasoactive peptides has been explored previously [76]. However, this is the first attempt to use a genetically encodable neuronal activity sensor with capabilities of cell targeting that triggers an artificial hemodynamic response as the readout. For this principle to succeed one needs to reduce the endogenous BOLD signal which can be accomplished using pharmacological inhibition. The engineered NOS requires the following properties: i) a calcium activated enzyme that produces NO ii) higher inhibition constants for drugs that inhibit endogenous nNOS. Since our engineered NOS exhibits a different inhibition constant compared to endogenous nNOS, we call the engineered version NOSTIC (Nitric Oxide Synthase with Tailored Inhibition Constants).

3. DESIGN OF NOSTICS

There are at least three known mammalian nitric oxide synthases that play different functional roles in tissue [77]. Neuronal nitric oxide synthase (nNOS) is expressed in neurons, endothelial nitric oxide synthase (eNOS), is expressed in endothelial cells, and inducible nitric oxide synthase (iNOS) is expressed in macrophages during an immune response. All three isozymes are known to have at least three domains: i) catalytic (N-terminal) domain that binds L-arginine (substrate), iron protoporphyrin IX (heme), and (6R)-5,6,7,8-tetrahydrobiopterin (BH4) ii) calmodulin-binding domain (CBD) that binds Calmodulin (CaM), and iii) C-terminal domain that binds to co-factors nicotinamide adenine dinucleotide phosphate (NADPH), flavin adenine dinucleotide (FAD), and flavin mononucleotide (FMN). Of these, eNOS and nNOS have CBDs that

bind CaM in a calcium-dependent manner thereby making those isozymes calcium activated.

The inhibition profiles of these NOS enzymes are determined by their catalytic domains [79]. NOS inhibitors are often arginine analogues that inhibit substrate binding or molecules that inhibit binding of BH4 or heme. Specificity of certain inhibitors is determined by secondary contacts between the inhibitor and the catalytic domain [79]. Based on this structural information we proceeded to design NOSTIC candidates as chimeric proteins by domain swapping. This involves swapping the domains of NOS isozymes. A study investigating the calmodulin-binding domains of the three different enzymes had previously assembled similar chimeric proteins [80].

4. MATERIALS AND METHODS

4. A. DNA ASSEMBLY

The plasmid pCWori containing human iNOS (hiNOS) and rat nNOS (rnNOS) constructs were a generous gift from the lab of Dr. Thomas Poulos at University of California, Irvine. Bovine eNOS (beNOS) and human eNOS (heNOS) encoding plasmids were a generous gift from Dr. Paul Ortiz de Montellano at University of California, San Francisco. The rnNOS, hiNOS, heNOS, were individually cloned into the pIRESpuro3 mammalian vector (Takara, Cat #631619). An inverse polymerase chain reaction (iPCR) was performed to create the backbone. Inserts were amplified from the pCWori backbone using overhangs ranging from 24-30 nucleotides on each end. A single-step, isothermal, ligation-free procedure was used to integrate the inserts. The entire length of the coding strand was verified using sequencing. A similar DNA assembly strategy was used to

generate chimeric genes. To introduce point mutations in genes, primers were designed with either the forward or the reverse primer containing the intended mutation. Prior to iPCR, 5′ end of the primers were phosphorylated using T4 PNK (NEB, MO201S). Following PCR, the reaction mix was treated with DpnI (NEB, R0176S), and ligated using NEB Quick Ligase kit (M2200S).

4. B. CELL CULTURE, NOS ACTIVITY, INHIBITOR SENSITIVITY

293-F Freestyle cells (ThermoFisher, Cat. #R79007) were maintained according to the manufacturer's protocol. To test for expression and activity of NOS constructs, high-purity DNA was obtained using Qiagen's Maxiprep kit (Cat. #12162). DNA was introduced into the cells using 293Fectin (ThermoFisher, Cat. #12347019) following the manufacturer's protocols. 48 hours post-transfection, cells were pelleted and resuspended in Freestyle 293 Expression Medium (ThermoFisher, Cat. #12338018) containing 1 mM L-arginine (Sigma Cat. #A5006) and 1mM $CaCl_2$ (Sigma Cat. #C3306) and seeded in 6-well plates at 1million cells per well. Cells were stimulated with 5 μM A23187 (Sigma, Cat. #C7522). Catalytic activity of NOS constructs was determined by quantifying nitrite from the supernatant using the Griess reagent system (Promega, Cat. #G2930) following the manufacturer's protocol. For experiments to test for inhibitor sensitivity of different NOS constructs, the following inhibitors (where applicable) were added to resuspension medium prior to stimulation of the cells: i) NG-Nitro-L-arginine methyl ester hydrochloride (L-NAME, Tocris, Cat. #0665), ii) *N*-[4-[2-[[(3-Chlorophenyl)methyl]amino]ethyl]phenyl]-2-thiophenecarboxamide dihydrochloride (ARL17477, Tocris, Cat. #3319), iii) *N*-[[3-(Aminomethyl)phenyl]methyl]-

ethanimidamide dihydrochloride (1400W, Tocris, Cat. #1415), iv) 7-nitroindazole (7-NI, Sigma, Cat. #N7778).

4. C. TEST FOR EXPRESSION VIRALLY DELIVERED NOSTICS

48 hours post transfection or viral transduction of NOSTIC constructs, cells were pelleted and resuspended in RIPA buffer (ThermoFisher, Cat. #89900) containing Halt Protease Inhibitor Cocktail (ThermoFisher, Cat. #78430), and Benzonase Nuclease (Sigma, Cat. #E1014). Following incubation for 10 minutes on a nutator, the samples were centrifuged at 14000g for 15 minutes. Total protein concentration was determined using Pierce 660 assay (ThermoFisher, Cat. #22660). 10 μg of total protein were loaded on to 4-15% MiniPROTEAN Precast Gels (BioRad, Cat. #4561086) and transferred onto PVDF membranes (BioRad, Cat. #1620177). The membrane was blocked in 3% w/v dry milk solution for 30 minutes, followed by incubation of primary antibody for 1 hour, washed three times with tris Buffer Saline with 0.1% Tween20 (TBST) for 5 minutes each, followed by incubation of horse radish peroxidase (HRP) tagged secondary antibody, washed three times with TBST, and probed with a chromogenic substrate (BioRad, #1708235). The following primary antibodies were used with the prescribed dilutions: i) mouse anti-FLAG (1:1000, Sigma, F1804) and ii) Rabbit anti-mCherry(1:1000, Abcam, ab167453). The following secondary antibodies were used with the prescribed dilutions: i) Donkey anti-mouse HRP (1:5000, Abcam, ab6820), ii) Donkey anti-rabbit HRP (1:5000, Abcam, ab6802).

4.D. TEST FOR CATALYTIC ACTIVITY OF VIRALLY DELIVERED NOSTICS

200,000 HEK 293FT cells were seeded on poly-D-lysine and laminin coated coverslips (Fisher Scientific, Cat. #08774385) in a 24-well plate. The following day, 1 μL

of 10^9 pfu/ml herpes simplex virus (HSV) delivering NOSTIC-2 or mCherry was added to each well. 24-48 hours later, media was aspirated, washed, and the cells were stimulated with 5 μM A23187 in 400μL (per well) Freestyle medium supplemented with 1 mM $CaCl_2$. Nitrite was quantified from supernatants using the Griess assay following overnight stimulation.

4.E. *IN VIVO* EXPERIMENTS

My colleague Dr. Nan Li carried out the *in vivo* experiments. Experiments were performed according to Massachusetts Institute of Technology (MIT) Committee on Animal Care rules, and in accordance with the institutional and National Institutes of Health (NIH) guidelines. Male Sprague-Dawley rats (180-200g) purchased from Charles River Laboratories were housed and maintained on a 12 h light/dark cycle with *ad libitum* access to food and water. Herpes simplex virus (HSV) vectors HSV-hEF1a-NOSTIC-2-IRES-mCherry or HSV-hEF1a-mCherry driven by the human elongation factor (EF1α) promoter were stereotaxically injected to the rat striatum (6 μL, AP 0 mm, ML 3.0 mm, DV 5 – 6mm). Approximately three weeks after viral injection, the rats were imaged under medetomidine anesthesia in response to median forebrain bundle stimulation ipsilateral to the viral injection site. Imaging data were acquired on a 9.4 T MR scanner (Bruker, Germany) using T_2*-weighted echo planar imaging (EPI) sequences for detection of stimulus-induced BOLD contrast. In order to discern NOSTIC-2-dependence of the resulting functional hemodynamic imaging signals, these experiments were performed under two successive conditions: (1) in the absence of any vasoactive drugs, (2) in the presence of 1400W, an inhibitor chosen to suppress NOSTIC-2-induced

fMRI signals. Control group of animal with viral vectors HSV-hEF1a-mCherry was tested under the same two imaging conditions as described above.

4. F. IMMUNOHISTOCHEMISTRY

Rats injected with HSV-hEF1a-NOSTIC-2-IRES-mCherry were perfused with 4% paraformaldehyde (PFA) and then fixed in PFA for 48 hours at 4°C. 50 μm free-floating sections were obtained using a semi-automatic vibratome (LeicaVT1200, Leica). Slices were stored in phosphate buffer saline (PBS, ThermoFisher, Cat. #10010023) at 4°C. Prior to staining, slices were washed thrice in PBST (PBS + 0.1% TritonX) and blocked for 1 hour with 10% v/v donkey serum (Sigma, D9663). Each slice was then incubated overnight at 4°C with gentle shaking in PBST with 1% donkey serum and anti-mCherry primary antibody (1:200, Abcam, ab167453). The following day, cells were washed thrice with PBST and then probed with an Alexa Fluor 594 conjugated secondary antibody (1:500, Abcam, ab150076) in PBST with 1% donkey serum for 1 hour. Slices were then washed thrice in PBS, mounted on glass slides with Prolong antifade mountant (ThermoFisher, P36962) and imaged on a confocal microscope.

5. RESULTS

5.A. ASSAY TO TEST NOS VARIANTS

We developed a cell-based assay similar to the one previously described [81]. Following transfection of various NOS variants, we seeded cells in a 6-well plate and stimulated them with 5 μM A23187. Nitrite content from supernatants was measured at the end of 2, 4, 6, and 8 hours (Fig 1A, B, C). Control transfection of GFP along with no stimulation controls at the end of 8 hours is shown in Fig 1D.

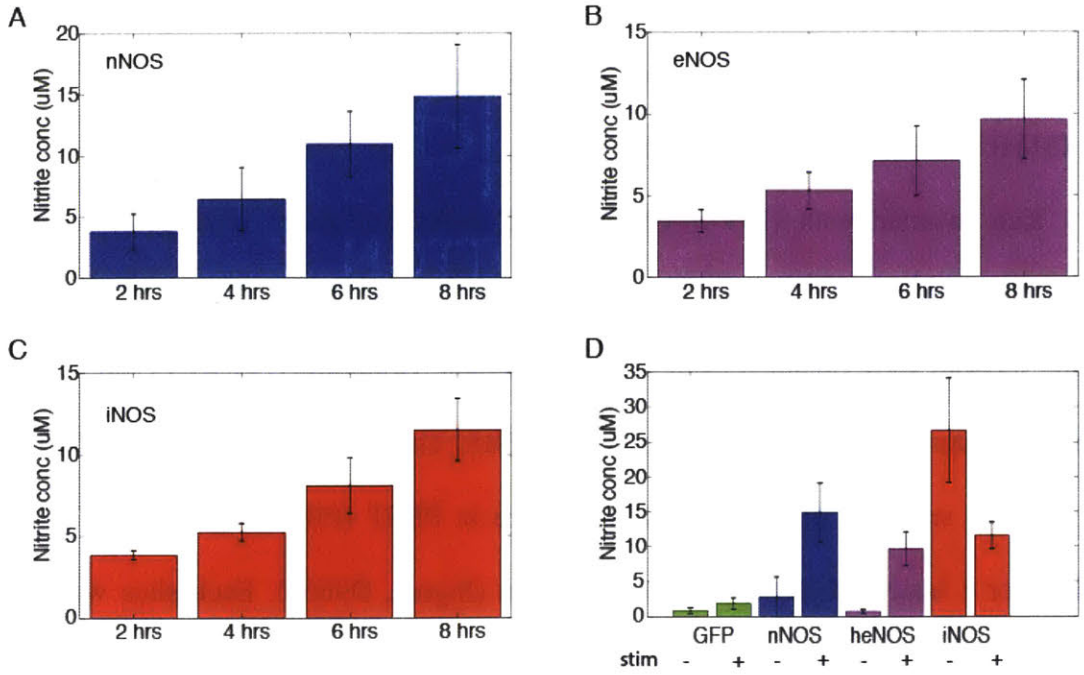

Fig 2. Time-dependence of catalytic activity as measured by quantifying nitrite using Griess reagent for nNOS (A), eNOS (B), iNOS (C). D) Comparison of catalytic activity of GFP (control), nNOS, eNOS, and iNOS measured after 8 hours of stimulation with 5 μM A23187 (+) or no stimulation (-). Error bars represent standard deviations (n=3).

We observed calcium dependent catalytic activity for both nNOS and eNOS. We collected time points to be able to determine a good dynamic range for the assay. Since at 8 hours, all the NOS variants tested had about 10 times the activity of the detection limit (1 μM) for the test, we subsequently tested catalytically activity 8 hours post-stimulation. It is important to note that iNOS whose catalytic activity is calcium-independent shows higher activity in the unstimulated condition than when stimulated. We use this assay to test engineered potential NOS variants with altered inhibition constants.

5.B. CALCIUM DEPENDENT ACTIVITY OF NOSTICS

To design NOSTICS, a number of possibilities were explored: i) swapped in the calmodulin binding domain of eNOS with iNOS to generate iNOS1-504eNOS489-

512iNOS532-1153 and iNOS1-504eNOS493-512iNOS532-1153, ii) swapped in the calmoduin binding domain of nNOS within iNOS to generate iNOS1-504nNOS725-754iNOS532-1153 and iNOS1-504nNOS732-754iNOS532-1153, iii) assembled chimeric NOS with the oxygenase domain of iNOS and the calmoduin binding domain and reductase domain of nNOS to form iNOS1-500nNOS703-1429 and iNOS1-504nNOS723-1429, and iv) assembled chimeric NOS with the oxygenase domain of iNOS and the calmoduin binding domain and reductase domain of eNOS to form iNOS1-504eNOS489-1203. The numberings mentioned here are amino acid numbers for rat nNOS, human iNOS, and human eNOS. The iNOS1-500nNOS703-1429 and iNOS1-504nNOS723-1429 were found to be the two promising candidates in terms of absolute catalytic activity and were renamed as NOSTIC-1 and NOSTIC-2 respectively (Fig 2A) Since the nNOS has a PDZ domain in its N-terminus, we assembled a PDZ-NOSTIC-2 construct with nNOS1-226iNOS1-504nNOS723-1429. All of the engineered NOS constructs had a C-terminal FLAG tag. The catalytic activities of these engineered constructs are shown in Fig 2A. Since any potential NOSTIC candidate needs to demonstrate calcium-dependent activity we tabulated the ratio of nitrite formation when stimulated with 5 μM A23187 to the unstimulated condition in Fig 2B.

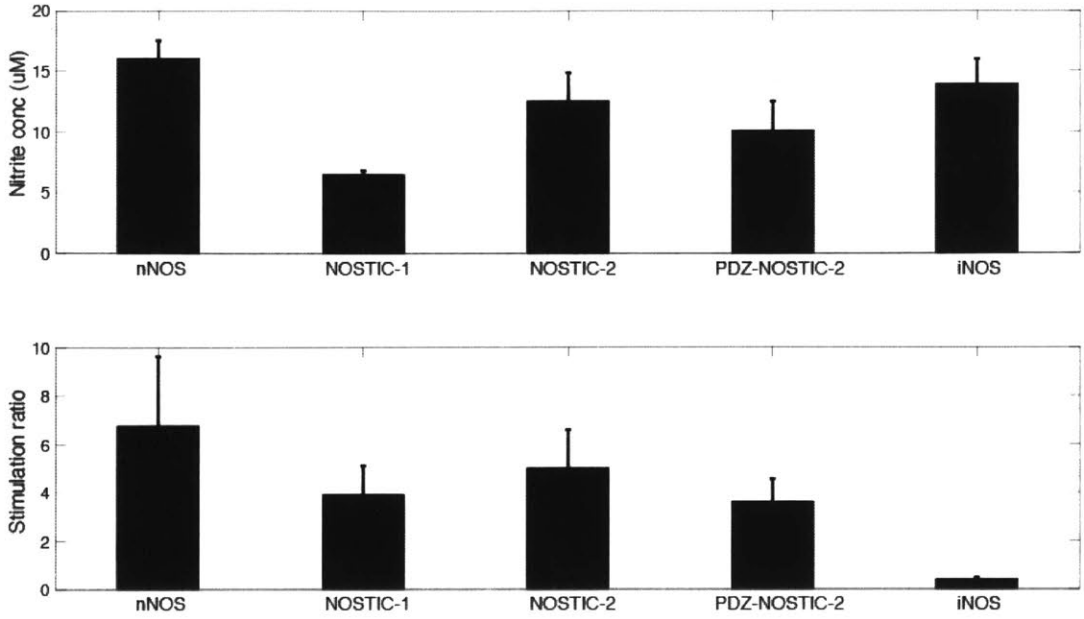

Fig 2. A.) Comparison of catalytic activity of NOSTICs along with nNOS and iNOS upon stimulation with 5 μM A23187. B.) Comparison of calcium-dependent activity as measured by nitrite production upon stimulation to nitrite production in absence of stimulation. Error bars represent standard deviation from at least three independent experiments.

Ideally, we would prefer any engineered NOS to be as catalytically active as endogenous nNOS. From our preliminary screen, NOSTIC-2 exhibited ~75% of the catalytically activity as nNOS and we proceeded to estimate the inhibition constants of NOSTIC-2 for ARL17477, L-NAME, and 1400W.

5.C INHIBITOR SENSITIVTY OF NOSTICS

We generated the inhibitor sensitivity profile of NOSTIC-2 for iNOS-specific inhibitor 1400W, non-specific inhibitor L-NAME, and nNOS-specific inhibitor ARL1477 and compared them to inhibitor sensitivity profiles of nNOS and iNOS. As expected, NOSTIC-2 had a similar inhibition profile to iNOS for 1400W (Fig 3A). NOSTIC-2 had a 5-fold higher IC_{50} for L-NAME compared to nNOS (Fig 3B) and a 10-fold higher IC_{50} for ARL17477 (Fig 3C). Encouraged by these results we performed a

round of mutagenesis on NOSTIC-2 particularly at position T121 based on an earlier study [79]. We made the following four mutations T>S, T>K, T>D, T>F. The T>S was a similar mutation whereas we expected the other three to have some effect on ARL17477 inhibition. Based on inhibition studies with ARL17477, our best candidate was T121F denoted as NOSTIC-3 in Fig 3D. We further proceeded to do another round of mutagenesis on R266 but the subsequent mutants severely reduced the overall catalytic activity of the enzyme.

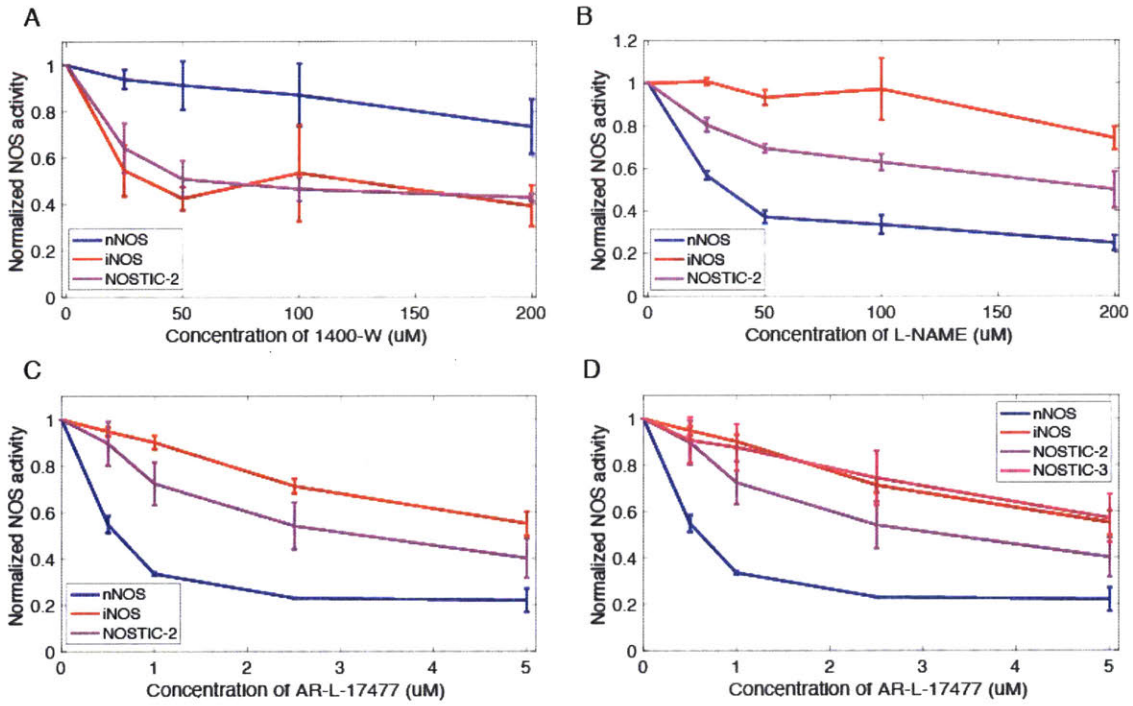

Fig 3. Inhibition profiles of nNOS, NOSTIC-2, and iNOS tested with 1400-W (A), L-NAME (B), AR-L-17477 (C). D.) Inhibition profiles NOSTIC-3 compared to NOSTIC-2, iNOS, and nNOS. Each measurement was made in triplicate and normalized to the activity with no drug added for each construct for each day. Error bars represent standard deviation.

5.D. ACTIVITY AND EXPRESSION TEST OF VIRALLY DELIVERED NOSTIC

The following constructs were packaged into herpes simplex virus (HSV) vectors by the Dr. Rachael Neve of the Gene Delivery Techonology Core at the Masschusetts

General Hospital i) HSV-hEF1a-mCherry and ii) HSV-hEF1a-NOSTIC-2-IRES-mCherry. We tested the virally delivered genes for catalytic activity and expression in HEK293FT cells and compared them to a corresponding transfection experiment. We confirmed the expression of NOSTIC-2 delivered by HSV using western blot and probing with anti-FLAG antibody (Fig 4A). We confirmed the catalytic activity of virally delivered NOSTIC-2 by quantifying nitrite formation using the Griess assay (Fig 4B).

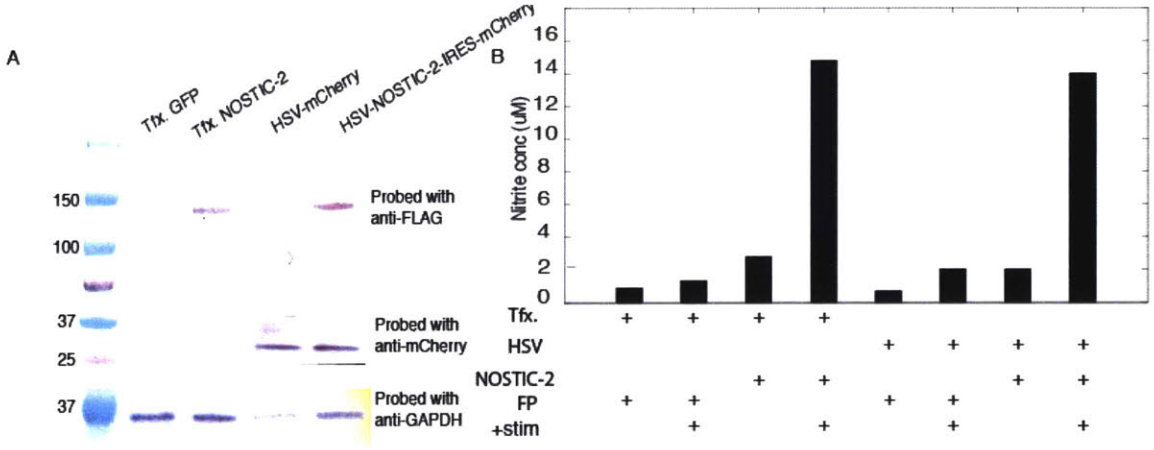

Fig 4. A) Western blot of transfected (Tfx) NOSTIC-2 or control (GFP) and virally delivered NOSTIC-2 and mCherry (control). Expected sizes: NOSTIC-2, 140kD; mCherry 29kD; GAPDH 37kD. B.) Catalytic activity of transfected NOSTIC-2, transfected GFP (control), virally delivered NOSTIC-2, virally delivered mCherry (control) in presence and absence of stimuli.

5.E. SMALL ANIMAL MRI OF VIRALLY DELIVERED NOSTIC

We then proceeded to test if virally delivered NOSTIC-2 could trigger a hemodynamic response that was detectable by MRI. We observed an increase in BOLD signal in the caudate putamen (close to site of injection) following MFB stimulation in rats injected with either NOSTIC-2 or mCherry. There was a decrease in signal following the addition of the iNOS inhibitor 1400W (Fig. 5). NOSTIC-2 having the iNOS catalytic domain was shown to be sensitive to 1400W. A pair wise Student's t-test showed the

difference in decrease in signal following addition of drug between NOSTIC-2 and mCherry injected rats to be not significant ($p = 0.08$).

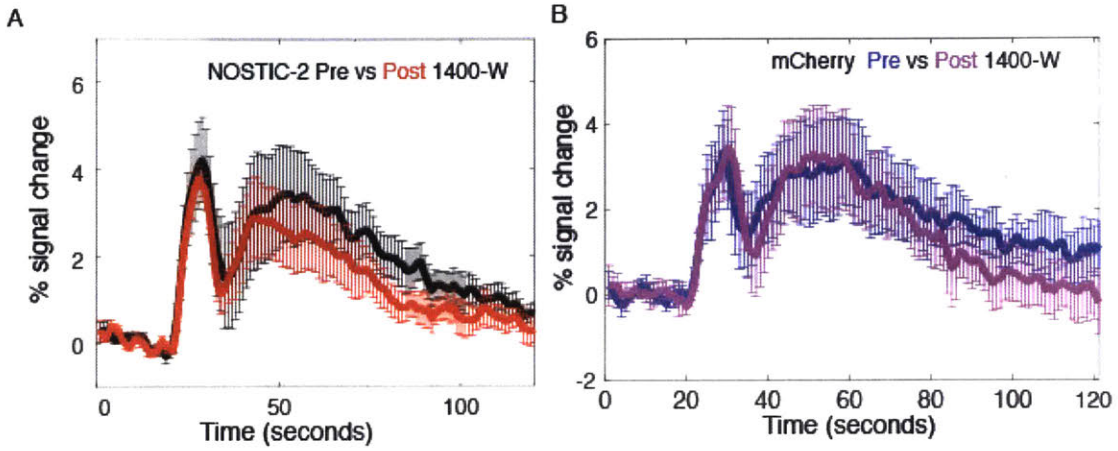

Fig 5. BOLD signal change from *in vivo* MRI scans of rats injected with virally delivered NOSTIC-2 (A) and mCherry (B). Pre represents signal change in response to MFB stimulation prior to 1400W injection and post represents BOLD response after 1400W treatment. Data shown here are responses from 5 animals.

We did not observe a significant signal increase overall from the NOSTIC-2 side post-stimulation but pre 1400W injection. It is possible that a combination of injury or immune response could have interfered with the hemodynamic response from NOSTIC-2. We therefore decided to look at regions away from the injection site that are connected to the striatum. One of these regions was the motor cortex (Fig 5A) where we see mCherry expression from our hEF1α-NOSTIC-2-IRES-mCherry construct. Comparing the response amplitudes to MFB stimulation we observed a significant increase in the NOSTIC-2-injected rats compared to mCherry-injected rats (Fig 5B, C).

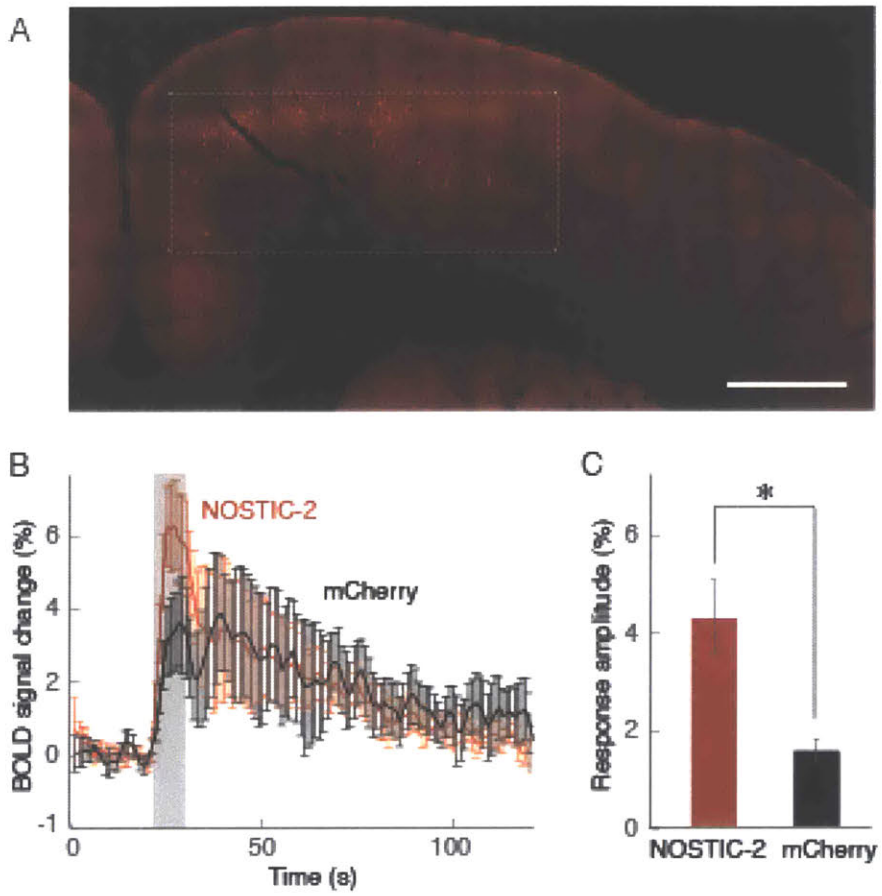

Fig 6. A.) Motor cortex of a rat injected with hEF1α-NOSTIC-2-IRES-mCherry construct. B.) Time courses of BOLD signal change in response to MFB stimulation in rats injected with mCherry (black) and NOSTIC-2 (red). C.) Comparison of response amplitudes between mCherry (black) and NOSTIC-2 (red) from at least 4 animals. An unpaired Student's t-test shows significant difference mCherry and NOSTIC-2 ($p = 0.01$). Scale bar is 1 mm.

6. DISCUSSION

In this study, we have developed a framework to design and test engineered nitric oxide synthases. In this case we demonstrated engineered NOS that exhibit calcium dependent catalytic activity like eNOS and nNOS but have inhibitor sensitivities to known NOS inhibitors like L-NAME and ARL17477 similar to that of iNOS. This

illustrates that swapping out domains of nitric oxide synthases is a viable strategy to engineer NOSTIC.

We have shown that point mutations could complement the domain swapping strategy to further fine tune inhibition constants against specific inhibitors. This strategy combined with the assay to test for NOS activity can be used to potentially modify other properties such as calcium sensitivity or even engineered NOS with alternate substrates. It is also worth noting that efforts in this study focused on tailoring the inhibition constant of NOSTICs to be more like iNOS and unlike nNOS. eNOS has a role to play in the hemodynamic response and hence it could be a fascinating to study if NOSTICs are more useful with inhibition constants similar to eNOS or different from eNOS.

Much like nitric oxide synthases, NOSTICs are large (3.7kb) constructs and hence difficult to package in Adeno associated virus (AAVs). This represents a serious bottleneck for technologies based on NOS/NOSTIC. While HSV can easily package larger genes, the possibility of an immune response cannot be ruled out. This is somewhat important particularly in this case, as presence of any endogenous iNOS would mask the effect of NOSTICs and potentially represent a decrease in BOLD signal following application of 1400W that is not NOSTIC-dependent. On the other hand, there is no denying that a retrograde virus (e.g. HSV) opens numerous possibilities in terms of being able to record from locations sway from the injection site. This strategy has not yet been fully explored and offers possibilities particularly if there is sufficient delivery of NOSTIC in remote regions.

This study represents a significant step forward towards the goal of being able to associate cell populations with neural activity recording from a whole brain in rodents.

Moreover it provides a platform upon which improvements to NOSTIC can be designed and tested. There is still the opportunity to improve the overall catalytic activity of NOSTICs and make it more comparable to nNOS. This maybe achieved with some fine-tuning of the region where the iNOS catalytic domain is fused with the nNOS calmodulin-binding domain. It is possible that the most efficient NOSTIC activity *in vivo* is achieved by a NOSTIC with a PDZ domain in which case it is worth improving upon the PDZ-NOSTIC-2. While this study focuses on the protein engineering aspects there are also possibilities to develop cell-permeable nNOS specific inhibitors not used in this study. Overall, NOSTICs offer unique opportunities towards generating a genetically encodable calcium sensor for MRI.

A MODULAR PLATFORM FOR VISUALIZING NEUROBIOLOGICAL SIGNALING USING MRI

1. ABSTRACT

Functional magnetic resonance imaging (fMRI) allows us to map localized changes in blood flow and volume and by extension the physiological phenomenon of vasodilation. Nitric oxide, a freely diffusible gas, is a chemical messenger that triggers vasodilation. Nitric oxide is a product of the enzyme nitric oxide synthase (NOS). In this study we demonstrate that NOS delivered via engineered HEK cells produces sufficient NO to be detectable my MRI. We further demonstrate that these engineered cells could be used as a platform to study cellular signaling by engineering specific receptors along with NOS.

2. INTRODUCTION

With the advent of technologies that allow targeting genetic populations [82] along with improved genetically encoded calcium sensors [18] and actuators [83] a significant portion of the efforts in dissecting the workings of the brain has shifted to cell-types and circuits. While this approach has its unique advantages [84], it is worthwhile remembering that brain function is not merely a set of polarization/depolarization events but also a system of complex neurotransmission. Neurotransmitters play key roles in development [84], cognition [85], memory [86], and have been implicated in a number of diseases [87, 88]. Thus to have a full breadth of the workings of the brain and in particular neurobiological signaling dynamics tools that help us visualize neurotransmission in real time is essential.

The circular permuted GFP (cpGFP) [89] has been the basis for multiple calcium sensors [90]. It was incorporated in sensors to visualize both glutamate [91] and γ-amino butyric acid [92] dynamics in zebra fish and mice. Recently two separate groups reported fluorescent sensors that were used visualize dopamine dynamics *in vivo* [93, 94]. Efforts in the Jasanoff lab have been directed towards recording neurotransmitter dynamics using MRI. These efforts aim to record from deep brain regions over a field of view that is currently out of reach for optical imaging or electrical recordings. Lee *et al.* [67] quantified dopamine release in nucleus accumbens in response to electrical stimulation in the median forebrain bundle while Hai *et al.* modeled serotonin reuptake and the how it is affected by selective serotonin reuptake inhibitors. One of the key components of these two studies was the availability of MRI-detectable dopamine and serotonin sensor respectively.

In this study we harness the usefulness of hemogenetic imaging described previously and try to leverage it as a platform for neurotransmitter sensor. To achieve this we first engineer human embryonic kidney (HEK 293FT) cells stably expressing nNOS (HEK-nNOS). We demonstrate that delivering nNOS via HEK cells in the rat striatum and stimulating them with A23187 is sufficient to detect NOS activity by BOLD MRI. We then use these stably expressing nNOS cells and engineer them to express adrenergic receptor (α_1AR). We show that norepinephrine (NE) can be used to trigger NOS activity in cells stably expressing both nNOS and A1αR (HEK-nNOS-α_1AR). This cell-based neurotransmitter sensor is conceptually similar to the fluorescent constructs described in previous work [95, 96]. However, it is intentionally designed to be compatible with MRI

to so it can be issued for deep brain imaging and potentially to study connectivity maps of distant areas in the brain.

3. MATERIALS AND METHODS

3. A. DNA ASSEMBLY

A lentiviral backbone with CMV promoter driving eGFP with a Blasticidin resistance cassette driven by a PGK promoter was used to generate pLV6-nNOS-BLA. pLV6-eGFP was treated with BamHI (NEB, Cat. #R0136S) and EcoRI (NEB, Cat. #R0101S) to make linearized vector. nNOS was amplified using polymerase chain reaction (PCR) with primers having 20-25bp overhang. The purified PCR product and the linearized backbone were assembled using Gibson assembly [97]. DNA was transformed in Stable competent cells (NEB, Cat. #3040I). The entire length of the coding sequence was verified by sequencing. The α_1AR coding strand with a V5 epitope tag was ordered as g-block fragment from IDT. It was amplified using PCR with primers having 20-25bp overhang. Gibson assembly was used to clone it into a lentiviral backbone with PGK promoter driving a Puromycin resistance cassette to generate pLV6-α_1AR-puro.

3. B. CELL CULTURE, STABLE LINE GENERATION

293FT cells (ThermoFisher, Cat. # R70007) were maintained in accordance with manufacturer's guidelines. Cells were co-transfected with pLV6-nNOS-BLA, psPAX2, and pMD2.G (Addgene) using Lipofectamine 3000 (ThermoFisher, Cat. #L300001). 48 hours post-transfection the supernatant containing lentiviral particles were added to freshly seeded cells on a 10-cm tissue culture dish. 24-hours following the addition of the lentiviral supernatant, the media was aspirated and changed with fresh media (DMEM

(ThermoFisher, Cat. #10569010) with 10% FBS (ThermoFisher Cat. #16000044) containing 10 μg/ml blasticidin. Media was changed every 48 hours till the dish was about 80% confluent. To generate cells stably co-expressing nNOS and α_1AR a similar strategy was used. In this case lentiviral particles containing α_1AR were added to stably expressing nNOS cells. To select for α_1AR, media supplemented with 10 μg/ml blasticidin and 1 μg/ml puromycin was used.

3. C. WESTERN BLOT

Stably expressing nNOS or nNOS and α_1AR cells were treated with radioimmunoprecipitation assay RIPA buffer (ThermoFisher, Cat. #89900) containing Halt Protease Inhibitor Cocktail (ThermoFisher, Cat. #78430), and Benzonase Nuclease (Sigma, Cat. #E1014). Following incubation for 10 minutes at room temperature, the samples were centrifuged at 14000g for 15 minutes. For testing for expression of α_1AR, we did not clarify the lysate as the protein is expected to be membrane bound. We therefore diluted the whole lysate is Lameli SDS-gel running before. Total protein concentration was determined using Pierce 660 assay (ThermoFisher, Cat. #22660). 10 μg of total protein were loaded on to 4-15% MiniPROTEAN Precast Gels (BioRad, Cat. #4561086) and transferred onto PVDF membranes (BioRad, Cat. #1620177). The membrane was blocked in 3% by weight dry milk solution for 30 minutes, followed by incubation of primary antibody for 1 hour, washed three times with tris buffer saline with 0.1% Tween20 (TBST) for 5 minutes each, followed by incubation of horse radish peroxidase (HRP) tagged secondary antibody, washed three times with TBST, and probed with a chromogenic substrate (BioRad, #1708235). The following primary antibodies were used with the prescribed dilutions: i) rabbit anti-nNOS (1:1000, Abcam,

ab76067) and ii) mouse anti-V5 (1:5000, ThermoFisher). The following secondary antibodies were used with the prescribed dilutions: i) Donkey anti-mouse HRP (1:5000, Abcam, ab6820), ii) Donkey anti-rabbit HRP (1:5000, Abcam, ab6802).

3. D. TEST FOR CATALYTIC ACTIVITY OF NOS

Either stably expressing nNOS or nNOS and α_1AR HEK cells were seeded on to either 6-well plate or 24-well plate at densities of 1 million per well or 20,000 per well respectively. The following day, cells were washed and then incubated in 2ml (for 6-well plate) or 400 µL (for 24-well plate) Freestlye medium supplemented with 1 mM $CaCl_2$. The cells were then stimulated with 0.1% DMSO (control), or 5 µM A23187, or 25 µM NE for 2 hours or 14 hours at 37°C. The supernatant was then used to quantify nitrite using the Griess reagent.

3. E. *IN VIVO* STUDIES WITH CELL INFUSION

My colleague Dr. Benjamin B. Bartelle performed the *in vivo* study. Experiments were performed according to Massachusetts Institute of Technology (MIT) Committee on Animal Care rules, and in accordance with the institutional and National Institutes of Health (NIH) guidelines. Male Sprague-Dawley rats, 8–10 weeks of age purchased from Charles River Laboratories were housed and maintained on a 12 h light/dark cycle with *ad libitum* access to food and water were used in this study. Prior to infusion HEK cells and nNOS-HEK cells were washed twice with PBS and then resuspended in artificial cerebrospinal fluid (aCSF) (Tocris Bio, Cat. #3525) at 1 million cells/µL. Rats were prepared for cell infusion as described in [98]. Rats were infused with 5 µL cells for 20 minutes. The location of the infusion was 0.7 mm anterior, 3 mm lateral, and 5 mm ventral to Bregma. The rats were scanned on a 9.4T magnet (Bruker) using a gradient

echo planar-imaging sequence. 50 μM A23187 was infused for a total volume of 1 μL over 5 minutes.

3. F. TEST FOR α_1AR ACTIVATION

To test for the activation of adrenergic receptor, HEK-nNOS-α_1AR cells were seeded in 96-well plates at 50,000 cells per well. The following day, media was aspirated and the cells were soaked in 5 μM Fura-2-AM (ThermoFisher, Cat. #F1201) diluted in OptiMEM (ThermoFisher, Cat. #31985062). Pluronic F-127 (ThermoFisher, Cat. #P3000MP) was added to increase dye retention. 75 minutes post incubation the cells were washed twice with Hank's Balanced Salt Solution (HBSS) (ThermoFisher, Cat. #14025076) and then stimulated with DMSO (vehicle control), 25 μM NE, or 10 μM Ionomycin (Sigma, Cat. #I0634) diluted in HBSS containing 1mM $CaCl_2$. We measured the fluorescence using a Spectramax M2 plate reader (Molecular Device) with excitation wavelengths set at 340 and 380 nm and emission wavelength set at 510 nm.

4. RESULTS

4. A. TEST FOR EXPRESSION AND CATALYTIC ACTIVITY OF nNOS

To test if we had cells stably expressing nNOS post blasticidin selection we performed a Western blot to test for expression. We observed a 160 kD band as expected (Fig. 1A). To test for catalytic activity, we stimulated cells with 5 μM A23187 diluted in Freestyle medium supplemented with CaCl2 for 14 hours and quantified nitrite formation. We observed catalytic activity from A23187 stimulated cells and not cells stimulated with the vehicle control, dimethyl sulfoxide (DMSO) and confirmed that our engineered cell line was stably expressing nNOS (Fig. 1B).

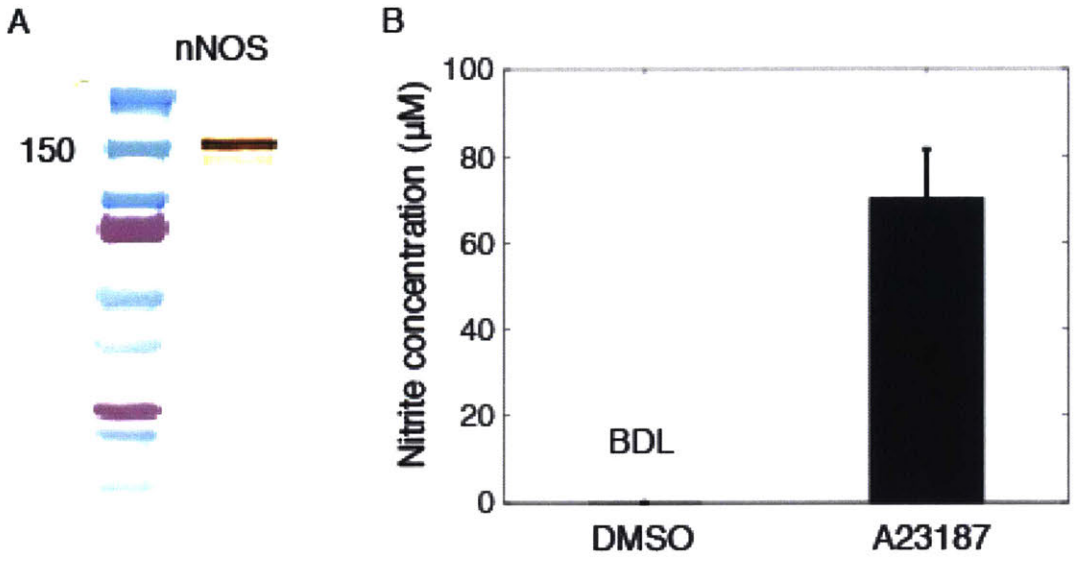

Fig 1. A.) Western blot of HEK-nNOS cells probed with anti-nNOS antibody. Expected band size: 160 kD. B.) Test for catalytic activity of HEK-nNOS cells as measured by Griess reagent upon stimulation with DMSO or 5 μM A23187. BDL: Below detection limit.

4. B. EFFECT OF ECTOPIC nNOS EXPRESSION *IN VIVO*

We wanted to see if stimulating HEK cells stably expressing nNOS *in vivo* displays sufficient catalytic activity to be detected by MRI. To test this we injected wild type HEK cells (control) and HEK-nNOS cells in opposing rat striata. A gradient echo planar imaging sequence was used to scan the animals in a 9.4 T scanner. We collected signal corresponding to 5 minutes of baseline activity followed by a 5-minute infusion of A23187 followed by another 5 minutes of recovery. We observed an elevated signal change on the side injected with cells that are stably expressing nNOS (Fig. 2). This result indicates that ectopically delivered nNOS when stimulated produces sufficient NO to be detected using MRI. This is important as this system could potentially be used as a platform to test for neurobiological signaling following more biologically relevant stimuli.

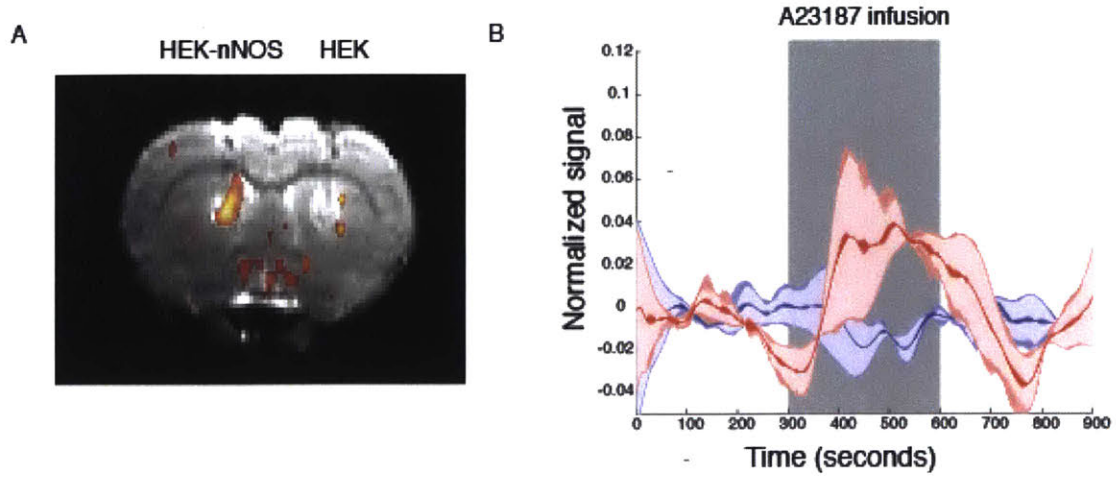

Fig. 2. A.) Brain slice showing area of injection of HEK-nNOS and HEK cells. B.) Time course of normalized signal from HEK cells (blue) and HEK-nNOS cells (red). The shaded area is grey denotes the time of stimulation with A23187. Data shown here are results are from imaging of two rats.

4. C. TEST FOR ACTIVATION AND EXPRESSION OF ADRENERGIC RECEPTOR

We used a similar approach to test for activation and expression of adrenergic receptor as we did for nNOS. Following selection with both blasticidin and puromycin, we performed a Western blot and independently probed for the expression of adrenergic receptor (via the V5 epitope tag) (Fig 3A) and nNOS using an anti-nNOS antibody (Fig 3B). To test for activation of the adrenergic receptor we used an intra-cellular calcium binding dye Fura-2-AM [99]. Activation of α_1 adrenergic receptors leads to activation of phospholipase C that produces intracellular calcium transients [100]. We observed an increase in F340/F380 ratio (excitation maxima of Fura-2 shifts to 340 nm from 380 nm in calcium bound state) upon stimulation with norepinephrine (Fig 3C). We measured the fluorescence for 15 minutes every 20 seconds. Data shown are from values at the end of 15 minutes.

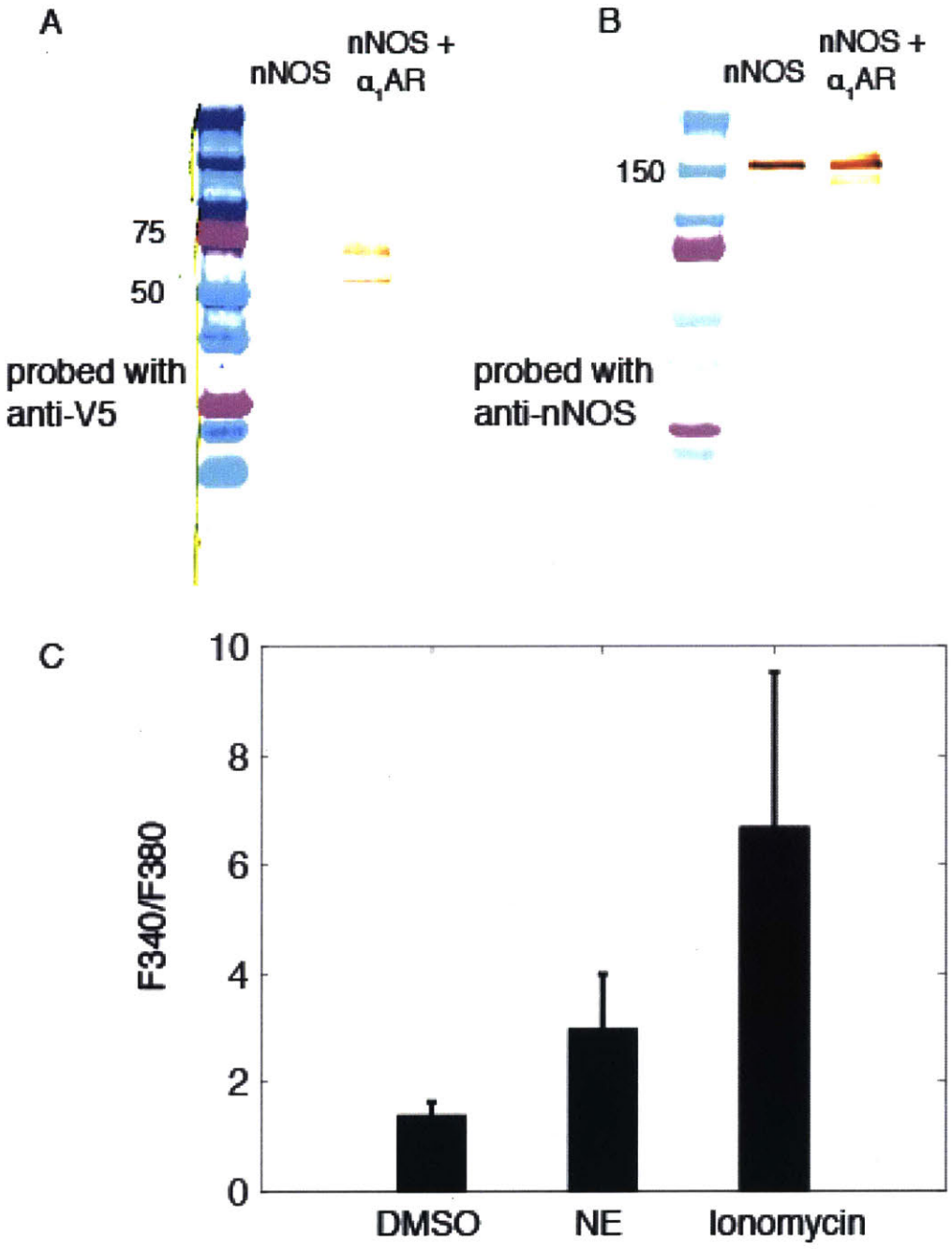

Fig. 3. Western blot of HEK-nNOS and HEK-nNOS-α_1AR cells probed with anti-V5 antibody (A) and anti-nNOS (B). Expected band size: nNOS 160 kD, α_1AR 53 kD. C.) Fura-2 assay to test for the activation of α_1AR with DMSO (control), 25 μM NE, 10 μM ionomycin. Measurements are shown from 4 independent experiments. Error bars represent standard deviations.

4.D. ACTIVATION OF nNOS WITH NOREPINEPHRINE

Our goal with this platform is to be able to visualize neurobiological signaling using MRI. We have thus far established that A23187 stimulation of HEK-nNOS can be visualized using MRI. So the next step was to test the activation of nNOS with a biologically relevant chemical messenger – norepinephrine.

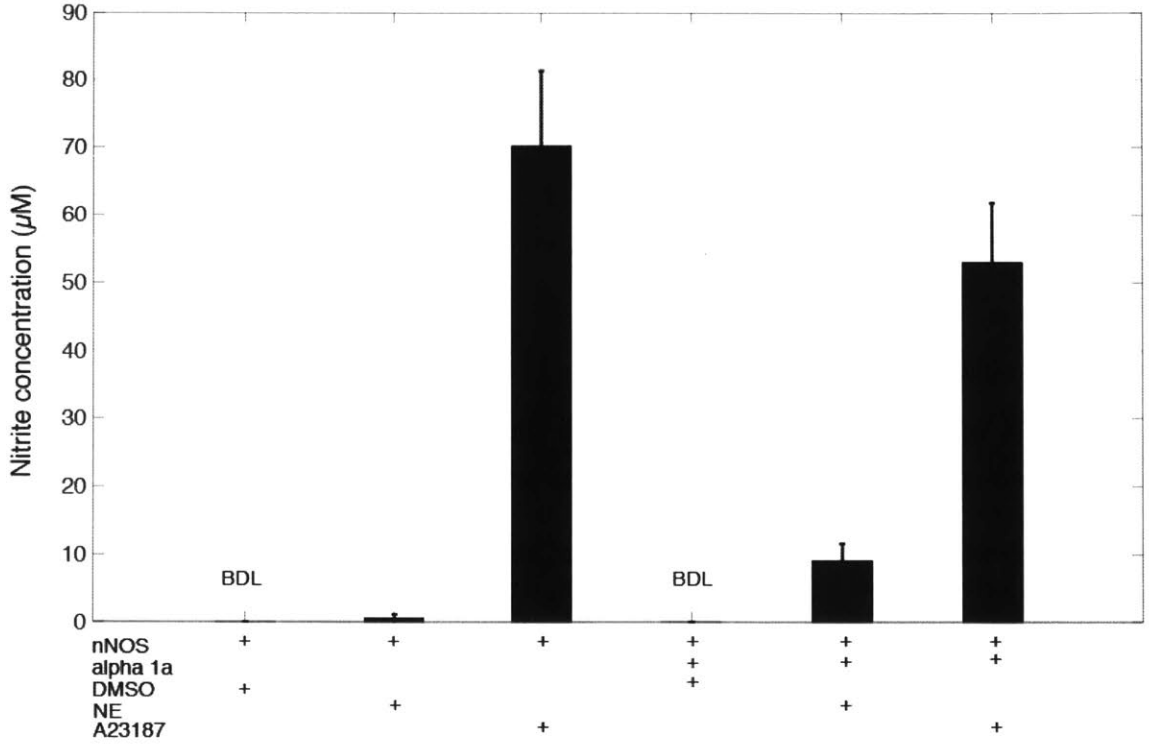

Fig 4. Activation of nNOS using NE in HEK-nNOS and HEK-nNOS- α_1AR cells. Data shown here are from three independent experiments. Error bars represent standard deviations.

We stimulated cells expressing both nNOS and α_1AR and cells expressing nNOS only with norepinephrine. We observed activation of nNOS using NE from cells expressing both the adrenergic receptor and nNOS but not from cells expressing nNOS only (Fig 4).

5. DISCUSSION

In this study we have demonstrated that catalytic activity of nNOS delivered through engineered HEK cells in a rodent brain can be detected using MRI. This system can be looked upon as a building block where the nNOS is the reporter. We could potentially add in a detector and use this platform to make a two-part sensor. We have also demonstrated that by using an adrenergic receptor we could detect catalytic activity of nNOS by norepinephrine stimulation. From our *in vivo* studies we could quantify the dosage of A23187 required to observe BOLD signal change. By comparing NOS activity triggered by an analyte of interest and comparing it to A23187 we could get an idea of the detection limit of that particular analyte *in vivo*.

While we look ahead to other molecules of interest one could potentially use this platform to build sensors for, it is worth remembering that since our readout leverages the hemodynamic response, molecules of interest that are themselves vasoactive could be difficult to detect *in vivo* or at least the dynamic range of their detection could be limited by our ability to separate signals coming from engineered cells or endogenous hemodynamic response. This is where NOSTICs could be potentially useful. If we replace nNOS in our system with a NOSTIC and then image in presence of an nNOS inhibitor -- this will likely help us diminish the BOLD signal from the endogenous hemodynamic response. This allows us to improve the existing technology in terms of diversifying the molecules of interest we could detect.

By combining this two-part platform with other actuators like electrical, photo, or chemogenetic stimulation it is possible to probe for connectivity of different parts of the brain with a higher amplification compared to regular BOLD signal. Perhaps a more

ambitious design could be to inject these sensors in more than one location and test if those regions of the brain are functionally connected both in resting state and in presence of stimuli.

This technology offers promising sensor design capabilities to study biological signaling.

ENGINEERING FERRITIN-BASED SENSOSRS FOR MOLECULAR IMAGING USING MRI

1. ABSTRACT

Conventional functional magnetic resonance imaging is dependent on the magnetic switching of hemoglobin. While hemoglobin in blood provides an endogenous source of contrast, visualizing specific molecular phenomenon based on the dynamics of the vasculature is complex. To study molecular phenomenon over a diverse time scale, more direct readout is required. Here we try to engineer a known MRI gene reporter, ferritin, to make molecular sensors based on it. We establish a screening system in *E. coli* that can be used to distinguish ferritin-fusion proteins by their ability confer iron scarcity in the cytosol. We then test candidates from this screening system in HEK cells and evaluate them for their ability to confer both expression-dependent and stimulus-dependent relaxivity changes in cells expressing them.

2. INTRODUCTION

MRI provides unique a unique opportunity to image molecular phenomenon in deep tissue [28]. fMRI has been the gold standard for whole brain imaging of neural activity. Due its dependence on blood flow the molecular phenomenon that can be probed with fMRI is somewhat limited [23]. Availability of analyte-sensitive MRI readable contrast agents would be useful in diversifying the molecular targets and the temporal precision with which their activities could be monitored [101]. Iron-oxide based superparamagnetic particles that couple the moments of a large numbers of ions provide great sensitivity as contrast agents. Examples of the use nanoparticles as MRI contrast agents can be found in [102].

Functionalized nanoparticles have been used to detect enzymatic activity [55] and calcium fluctuations both *in vitro* and *in vivo* [52, 53, 103]. While nanoparticle based contrast agents offer great contrast enhancement it is a challenge to deliver them. Targets of functionalized nanoparticles are usually limited to extracellular analytes. To engineer analyte-sensitive contrast agents that could be genetically targeted we need a genetically encodable MRI reporter. The potential of using ferritin, a multimeric iron-binding protein, as a gene reporter for MRI has been thoroughly investigated [56, 57, 58, 59]. However returns from efforts to visualize biological phenomenon using ferritin, as an MRI gene reporter have been modest [104, 105, 106]. Matsumoto and colleagues used directed evolution to screen from a library of 10^7 variants of ferritin (from *Pryococcus furiosus*) and obtained an engineered variant with twice the iron binding capacity as the wild type. This variant also demonstrated enhanced relaxation rates and analyte sensitivity in yeast [60].

Our goal was to use the output of that screen and try to engineer functionalized ferritins capable of sensing biomolecules of interest. Initial attempts to express functionalized ferritins in yeast yielded insoluble proteins. The ferritins we tested were N-terminally fused with calmodulin or hippocalcin. Hippocalcin belongs to the neuronal calcium sensor (NCS) class of proteins, expressed in the hippocampus. This protein exhibits a characteristic N-terminal myristoylation and undergoes a massive conformation change upon Ca^{2+} binding, which results in its translocation from the cytosol to the membrane [107]. Owing to our difficulty in getting functionalized ferritins to form in the cytosol of yeast we switched to an *E. coli* system where these fusion proteins were soluble. While functionalizing ferritins provide us the opportunity to

develop sensors based on it, it is conceivable that the iron-binding properties of the functionalized ferritins are altered. Therefore we needed a system to evaluate and eventually screen for improved iron binding of functionalized ferritins. We designed a screening system (Fig 1) based on the ferric uptake regulator (FUR), a protein that acts a repressor in its iron bound state [109]. We screened a number of iron-dependent promoters (Table 1) to construct a reporter plasmid with a fluorescent output on cytosolic iron scarcity. We used this reporter system to test ferritins from different

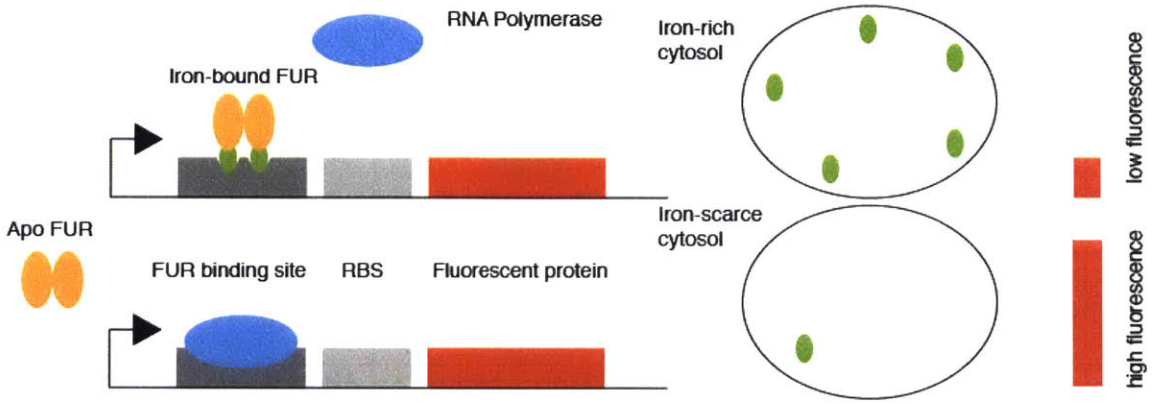

Fig 1. Schematic of the FUR-based reporter system in *E. coli:* under iron-rich conditions, FUR is iron-bound and acts as a repressor and hence gives a low fluorescence output. Under iron-depleted condition the apo-FUR no longer acts as a repressor and gives a high fluorescence output.

sources --- HFt: human heavy chain ferritin, PfFt: ferritin from *P. furiosus,* EcFtnA: ferritin from *E. coli,* ArchFt: ferritin from *A. fulgidus,* AA: double mutant of ArchFt reported to have a higher iron loading capacity [110, 111, 112, 113, 114]. Our assumption here was that cytosolic iron scarcity was a result of enhanced iron binding activity of ferritin or functionalized ferritins. We then tested functionalized ferritins for enhanced iron binding using the same reporter system and selected candidates were tested in HEK cells. We tested for both expression-dependent and stimulation-dependent changes in relaxivity.

3. MATERIALS AND METHODS

3. A. DNA ASSEMBLY

To build a reporter plasmid we used a p15A origin low copy plasmid expressing mCherry under a constitutive promoter with streptomycin resistance. The iron regulated

Name	Gene	-35		-10	
FUR 2	*FhuA*	TTGAGA	AAGATTCGCAATTT TTTGCT	GATAAT	GATAATCATTATC ACTAA
FUR 4	*aerobactin*	TTGATA	ATGATAATCATTAT TGA	CATAAT	TGTTATTATTTTAC ACTAA
FUR 5	*double box*	TTGATA	ATGATAATCATTAT TGA	GATAAT	GATAATCATTATC ACTAA
FUR 6	*fes*	TTGCAA	ATGCAAATAGTTAT CAT	TAATAT	TATCAATATATTT ACTAA
FUR 7	*entC*	TTGACA	TAGTGCGCGTTTGC TTT	TAGGTT	AGCGACCGAAAATATAAATG ATAATCATTAT
FUR 8	*cir*	TTGATA	ATTGTTATCGTTTG CAT	TATCGT	TACGCCGCAATCA ACTAA
FUR 9	*FhuF*	TTGATA	ATGATAACCAATAT CATAT	GATAAT	TTTTATCATTTGCAA ACTAA

Table 1: Operator sequences used to test iron-dependent expression of fluorescent proteins. Nucleotides in red are the expected FUR binding regions. -35 and -10 are numbers prior to the start codon.

operator/repressor sequences were cloned in as overhangs with iPCR. Prior to iPCR, 5′ ends of the primers were phosphorylated using T4 PNK (NEB, MO201S). Following PCR, the reaction mix was treated with DpnI (NEB, R0176S), and ligated using NEB Quick Ligase kit (M2200S). To test ferritins in conjunction with our reporter system, we cloned them in the pET28a plasmid (Millipore, Cat. #69864) under the T7 promoter and

the inducible lac operator using Gibson assembly [97]. To generate ferritin fusion proteins we also used a Gibson assembly strategy. For expression in HEK cells we used the pIRESpuro3 backbone (Takara, Cat. #631619) with ferritins or ferritin fusions driven by the cytomegalovirus (CMV) promoter.

3. B. TESTING LIBRARY OF FUR-BASED REPORTERS

Overnight cultures of *E. coli BL21DE3* (NEB, C2527I) cells harboring the reporter plasmids were diluted 1:100 and grown up to OD ~ 0.6 in lysogeny broth (LB) medium. They were then supplemented with either 40 μM ferrous ammonuim sulfate (FAS, Sigma, Cat. #203505) or 200 μM 2,2 dipryidyl (Sigma, D216305). Fluorescence measurements were made on a SpectraMax2 plate reader (Molecular Devices) at 6 hours and 20 hours post addition of iron/iron chelator.

3. C. TESTING FERRITIN CONSTRUCTS FOR IRON LOADING IN *E. COLI*

BL21DE3 cells selected for both a FUR-based reporter construct and ferritin/ferritin fusion construct was grown over night in LB with appropriate antibiotics. They were diluted 1:100 and grown up to O.D. 0.6-0.8. Ferritin for functionalized ferritin expression was induced using 1 mM isopropyl β-D-1-thiogalactopyranoside (IPTG). 5 hours post-induction, the cells were analyzed using flow cytometry (BD FACS LSR II, BD Biosciences) at the Koch Institute core facility at MIT.

3. D. RELAXOMETRY OF HEK CELLS

293-F Freestyle cells (ThermoFisher, R79007) were maintained according to the manufacturer's protocol. Prior to relaxometry, high-purity DNA of plasmids with ferritin or functionalized ferritin constructs was obtained using Qiagen's Maxiprep kit (Cat. #12162). DNA was introduced into the cells using 293Fectin (ThermoFisher, Cat.

#12347019) following the manufacturer's protocols. 24 hours post transfection cells were supplemented with either 1 mM ferric citrate (Sigma, F3388) or 1 mM ferrous ascorbate (Sigma, A0207). In some cases cells were co-transfected with a plasmid containing the divalent metal transporter (DMT1) gene. 48 hours post transfection cells were washed with Hanks' buffered saline solution (HBSS) twice and then plated onto 384 well plates. These were then scanned in a 7T magnet (Bruker). A multi spin multi echo sequence was used and R2 values were fitted using Matlab (Mathworks).

4. RESULTS

A. SCREENING OF FUR-BASED REPORTER SYSTEMS

Our mini library of FUR-based systems was derived from iron-regulated genes.

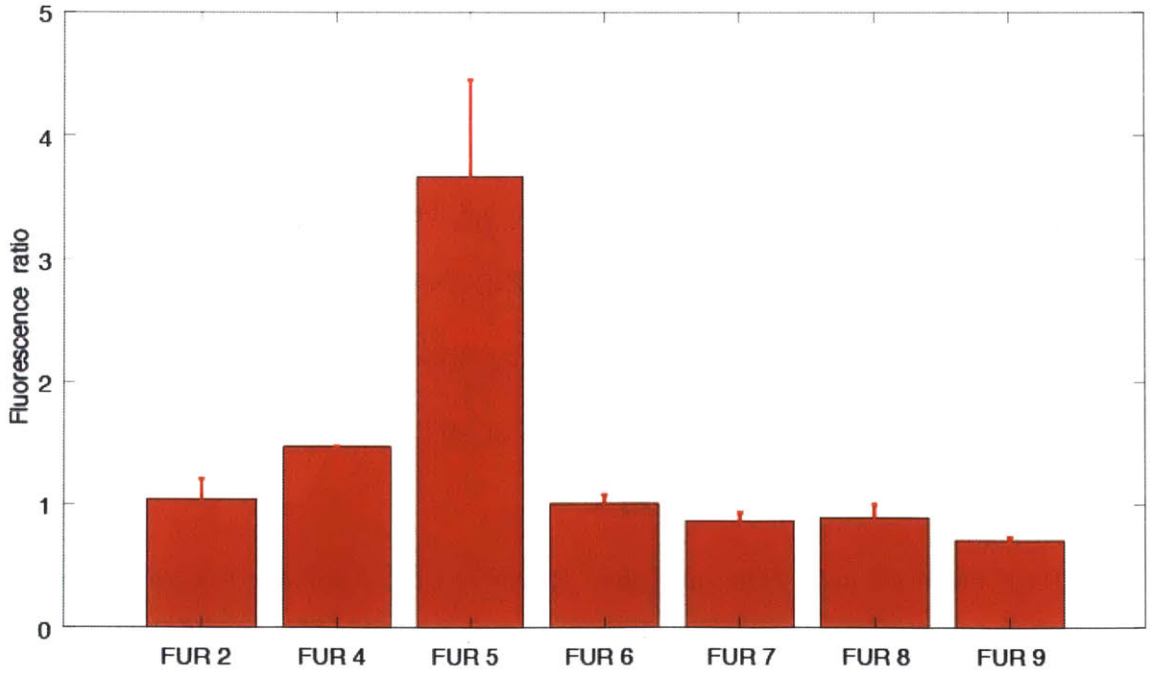

Fig 2. Comparison of FUR-based promoters: FUR 5 was the most promising candidate followed by FUR 4. These data are from three independent experiments. Error bars represent standard deviations.

FUR 2 was the same construct used in [114] although the E. coli strain used in this study is *BL21DE3* while theirs was *JM109*. Fluorescence output was calculated as a ratio of normalized fluorescence (normalized to O.D.) in presence of an iron chelator 2,2-dipyridyl to the normalized fluorescence in presence of supplemented ferrous ammonium sulfate. A synthetic promoter (FUR 5) with two potential FUR-binding sites gave the most promising output of an induction ratio of 3.8 (Fig. 2).

4. B. TESTING FERRITINS AND FUNCTIONALIZED FERRITINS FOR IRON BINDING

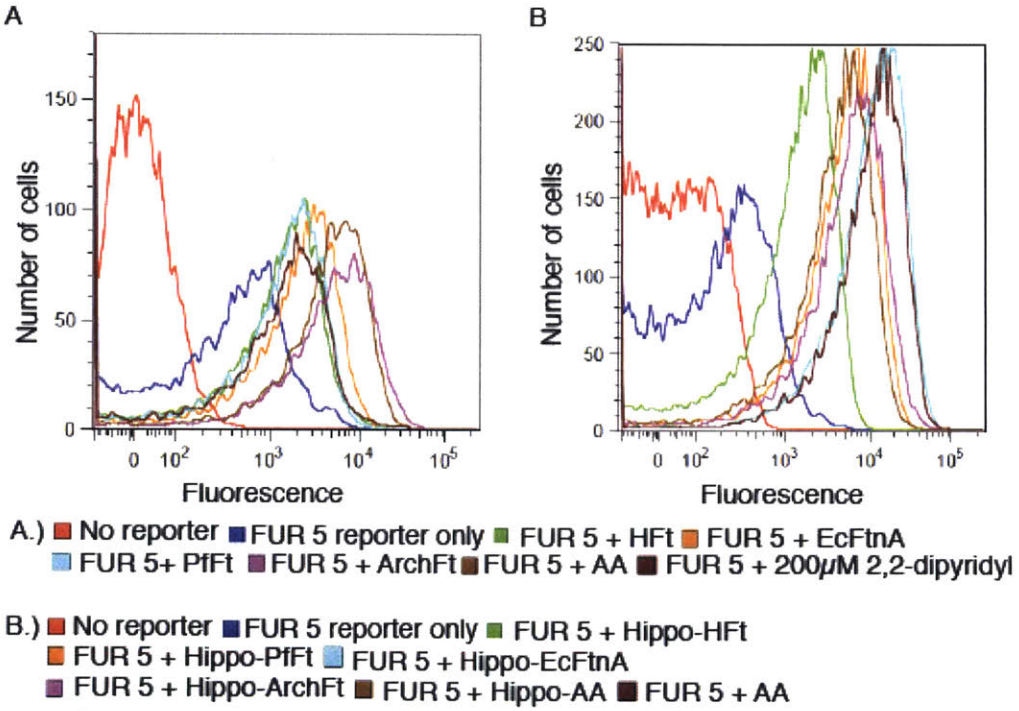

Fig 3. A.) Histogram from a flow cytometry experiment showing the effect of co-expressing ferritins along with FUR 5 reporter system. B.) Histogram from a flow cytometry experiment showing the effect of co-expressing hippocalcin-fused ferritins along with FUR 5 reporter system.

To test if our reporter system could distinguish between expression of ferritins from different sources, we co-expressed them with the FUR 5 reporter. We used the reporter-only as the negative control and FUR 5 reporter supplemented with 2,2-dipyridyl as the

positive control. We observed that among the ferritins tested, expression of ArchFt and AA showed maximum fluorescence increase (Fig 3A). We then tested for the ferritins functionalized with hippocalcin. For this experiment we used co-expression of FUR 5 with AA as the new positive control. Among the hippocalcin-fused ferritin, the hippo-EcFtnA was the most promising candidate. We hypothesized that candidates that displayed the best iron-binding phenotype is most likely to confer a higher R_2 when expressed in HEK cells.

4. C. RELAXOMETRY IN HEK CELLS

We co-transfected 293-F Freestyle cells with DMT-1 along one with one of Hippo-AA, Hippo-EcFtnA, Hippo-HFt, and mCherry (control). 24-hours post-transfection, 1mM Fe(II)-ascorbate was added to the medium and cells were incubated in them overnight. Cells were then washed, pelleted and imaged on a 7T magnet.

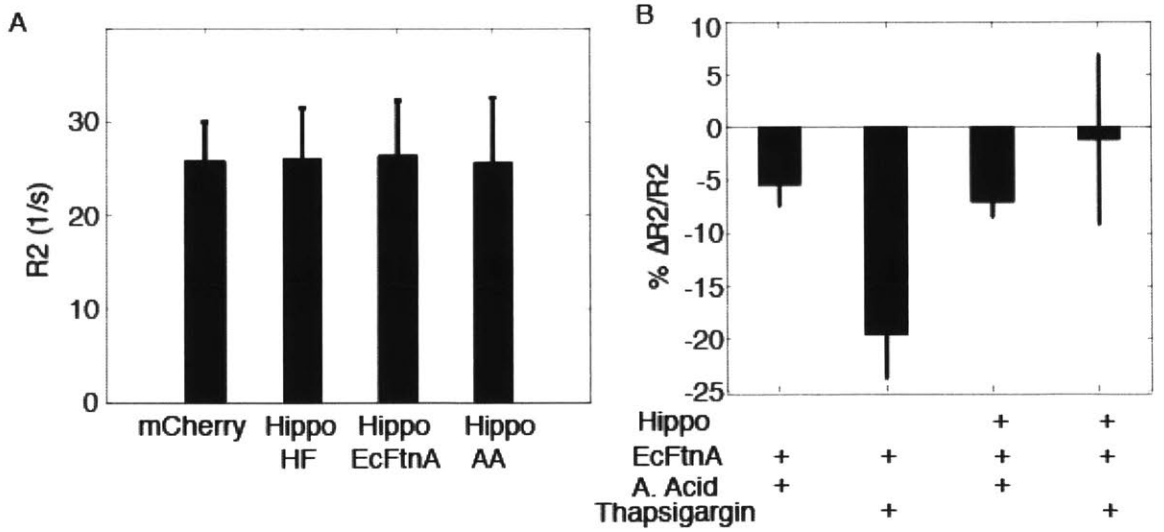

Fig 4. A.) Expression of neither of the hippocalcin fused ferritins exhibited higher relaxation rates than the control (mCherry). Data are from experiments with 2 replicated with each measurement made at least twice. B.) Stimulation of cells transfected with Hippo-EcFtnA or EcFtnA with arachidonic acid (30 μM) or thapsigargin (1 μM) revealed a significant decrease in R2 for EcFtnA only. Data shown are from two independent experiments experiments with each measurement made at least twice.

None of the functionalized ferritins performed any better than mCherry transfected HEK cells (control). To test for calcium-dependent R_2 changes we compared cells expressing hippocalcin-EcFtnA with EcFtnA alone. Compared to DMSO (control), thapsigargin stimulated EcFtnA cells showed significant decrease in R_2. This result is not intuitively obvious as thapsigargin is a Ca^{2+} ATPase blocker [115] that causes increase in cyctosolic calcium concentrations and as such should not affect the R_2 of EcFtnA not functionalized with a calcium-sensing domain.

5. DISCUSSION

In this study, we developed a reporter system that can report on the cytosolic iron levels in *E. coli*. We have further demonstrated that co-expression of ferritins from different sources can be distinguished using this reporter system. We have further shown that functionalized ferritins can be differentiated using this system. In general this system can be used as readout to study iron binding of cytosolic proteins. Our data further supports the idea that a reporter system like the one described could be used to evaluate and improve upon iron binding of functionalized ferritins.

In our case, we were most interested in ferritins as they represent a key starting point for building MRI readable sensors. Nanoparticles have already been demonstrated to work well as building blocks for MRI sensors [53]. Ferritins represent premier building blocks for intracellular analytes. While less magnetic they are genetically encodable. The complexity arises from ferritins by themselves not being magnetic without being iron bound. This necessitates the delivery of iron and it can almost be looked at as two-part system. Furthermore even in ferritin over-expressing

cells, not all iron supplementation necessarily finds its way to the ferritin [116]. We also tried tweaking parameters that might be useful in differentiating cells expressing ferritin compared to cells alone by relaxometry. This involved changing nature of chemical species supplemented (Fe (II) or (III)), incubation times, washouts, and not supplementing excess iron at all. However, we have not reliably seen an Ft-expression dependent *R2* change.

It is conceivable that if we could trigger an analyte dependent clustering of ferritin species and size of the clustered species were in the right range [117] we could see enhanced R_2 over cells expressing ferritins but without the induced clustering. Such a design would require a functionalization of ferritin not unlike the ones tried in this study. Such functionalization could lead to lower magnetic moment of the functionalized ferritins compared to their non-functionalized compartments. In such a scenario a reporter system like the one described here could be used to screen for higher iron binding among functionalized ferritins.

REFERENCES

1. Azevedo, F. A. C., Carvalho, L. R. B., Grinberg, L. T., Farfel, J. M., Ferretti, R. E. L., Leite, R. E. P., ... Herculano-Houzel, S. (2009). Equal numbers of neuronal and nonneuronal cells make the human brain an isometrically scaled-up primate brain. *The Journal of Comparative Neurology*, *513*(5), 532–541.
2. DeFelipe, J., Alonso-Nanclares, L., Arellano, J. (2002). Microstructure of the neocortex: comparative aspects. *Journal of neurocytology,* 31 (3-5), 299-316.
3. Jäkel, S., & Dimou, L. (2017). Glial Cells and Their Function in the Adult Brain: A Journey through the History of Their Ablation. *Frontiers in Cellular Neuroscience*, *11*,24.
4. Arellano, J. I., Benavides-Piccione, R., DeFelipe, J., & Yuste, R. (2007). Ultrastructure of Dendritic Spines: Correlation Between Synaptic and Spine Morphologies. *Frontiers in Neuroscience*, *1*(1), 131–143.
5. Brini, M., Calì, T., Ottolini, D., & Carafoli, E. (2014). Neuronal calcium signaling: function and dysfunction. *Cellular and Molecular Life Sciences*, *71*(15), 2787–2814.
6. Daneman, R., & Prat, A. (2015). The Blood–Brain Barrier. *Cold Spring Harbor Perspectives in Biology*, *7*(1), a020412.
7. Hodgkin, A. L., & Huxley, A. F. (1945). Resting and action potentials in single nerve fibres. *The Journal of Physiology*, *104*(2), 176–195.
8. Hamm, T. M., Sasaki, S., Stuart, D. G., Windhorst, U., & Yuan, C. S. (1987). The measurement of single motor-axon recurrent inhibitory post-synaptic potentials in the cat. *The Journal of Physiology*, *388*, 631–651.
9. Sayer, R. J., Friedlander, M. J., & Redman, S. J. (1990). The time course and

amplitude of EPSPs evoked at synapses between pairs of CA3/CA1 neurons in the hippocampal slice. *The Journal of Neuroscience : The Official Journal of the Society for Neuroscience*, *10*(3), 826–836.

10. Margrie, T., Brecht, M., & Sakmann, B. (2002). In vivo, low-resistance, whole-cell recordings from neurons in the anaesthetized and awake mammalian brain. *Pflugers Archiv European Journal of Physiology*, *444*(4), 491–498.
11. Kodandaramaiah, S. B., Franzesi, G. T., Chow, B. Y., Boyden, E. S., & Forest, C. R. (2012). Automated whole-cell patch clamp electrophysiology of neurons *in vivo*. *Nature Methods*, *9*(6), 585–587.
12. Shimomura, O. (1979). Structure of the chromophore of *Aequorea* green fluorescent protein. *FEBS Letters*, *104*(2), 220–222.
13. Pédelacq, J.-D., Cabantous, S., Tran, T., Terwilliger, T. C., & Waldo, G. S. (2006). Engineering and characterization of a superfolder green fluorescent protein. *Nature Biotechnology*, *24*(1), 79–88.
14. Zhang, G., Gurtu, V., & Kain, S. R. (1996). An Enhanced Green Fluorescent Protein Allows Sensitive Detection of Gene Transfer in Mammalian Cells. *Biochemical and Biophysical Research Communications*, *227*(3), 707–711.
15. Deliolanis, N. C., Kasmieh, R., Würdinger, T., Tannous, B. A., Shah, K., & Ntziachristos, V. (2008). Performance of the Red-shifted Fluorescent Proteins in deep-tissue molecular imaging applications. *Journal of Biomedical Optics*, *13*(4), 044008.
16. Livet, J., Weissman, T. A., Kang, H., Draft, R. W., Lu, J., Bennis, R. A., … Lichtman, J. W. (2007). Transgenic strategies for combinatorial expression of

fluorescent proteins in the nervous system. *Nature*, *450*(7166), 56–62.

17. Denk, W., Strickler, J. H., & Webb, W. W. (1990). Two-photon laser scanning fluorescence microscopy. *Science (New York, N.Y.)*, *248*(4951), 73–76.

18. Nakai, J., Ohkura, M., & Imoto, K. (2001). A high signal-to-noise Ca(2+) probe composed of a single green fluorescent protein. *Nature Biotechnology*, *19*(2), 137–141.

19. Mank, M., Reiff, D. F., Heim, N., Friedrich, M. W., Borst, A., & Griesbeck, O. (2006). A FRET-Based Calcium Biosensor with Fast Signal Kinetics and High Fluorescence Change. *Biophysical Journal*, *90*(5), 1790–1796.

20. Stirman, J. N., Smith, I. T., Kudenov, M. W., & Smith, S. L. (2016). Wide field-of-view, multi-region two-photon imaging of neuronal activity in the mammalian brain. *Nature Biotechnology*, *34*(8), 857–862.

21. Shukla, A. K., & Kumar, U. (2006). Positron emission tomography: An overview. *Journal of Medical Physics / Association of Medical Physicists of India*, *31*(1), 13–21.

22. Sokoloff, L., Reivich, M., Kennedy, C., Des Rosiers, M. H., Patlak, C. S., Pettigrew, K. D., ... Shinohara, M. (1977). The [14C]deoxyglucose method for the measurement of local cerebral glucose utilization: theory, procedure, and normal values in the conscious and anesthetized albino rat. *Journal of Neurochemistry*, *28*(5), 897–916.

23. Logothetis, N. K. (2008). What we can do and what we cannot do with fMRI. *Nature*, *453*(7197), 869–878.

24. Belliveau, J. W., Kennedy, D. N., McKinstry, R. C., Buchbinder, B. R., Weisskoff,

R. M., Cohen, M. S., ... Rosen, B. R. (1991). Functional mapping of the human visual cortex by magnetic resonance imaging. *Science (New York, N.Y.)*, *254*(5032), 716–719.

25. Logothetis, N. K., Guggenberger, H., Peled, S., & Pauls, J. (1999). Functional imaging of the monkey brain. *Nature Neuroscience*, *2*(6), 555–562.

26. Hall, W. A., Kim, P., & Truwit, C. L. (2008). Functional Magnetic Resonance Imaging-Guided Brain Tumor Resection. *Topics in Magnetic Resonance Imaging*, *19*(4), 205–212.

27. Van der Linden, A., Van Camp, N., Ramos-Cabrer, P., & Hoehn, M. (2007). Current status of functional MRI on small animals: application to physiology, pathophysiology, and cognition. *NMR in Biomedicine*, *20*(5), 522–545.

28. Ogawa, S., Lee, T. M., Nayak, A. S., & Glynn, P. (1990). Oxygenation-sensitive contrast in magnetic resonance image of rodent brain at high magnetic fields. *Magnetic Resonance in Medicine*, *14*(1), 68–78.

29. Ogawa, S., & Lee, T. M. (1990). Magnetic resonance imaging of blood vessels at high fields: in vivo and in vitro measurements and image simulation. *Magnetic Resonance in Medicine*, *16*(1), 9–18.

30. Ogawa, S., & Lee, T. M. (1990). Magnetic resonance imaging of blood vessels at high fields: in vivo and in vitro measurements and image simulation. *Magnetic Resonance in Medicine*, *16*(1), 9–18.

31. Bartelle, B. B., Barandov, A., & Jasanoff, A. (2016). Molecular fMRI. *The Journal of Neuroscience*, *36*(15), 4139–4148.

32. Flint, J. J., Lee, C. H., Hansen, B., Fey, M., Schmidig, D., Bui, J. D., ... Blackband, S. J. (2009). Magnetic Resonance Microscopy of Mammalian Neurons. *NeuroImage*, *46*(4), 1037–1040.

33. Lee, C. H., Blackband, S. J., & Fernandez-Funez, P. (2015). Visualization of synaptic domains in the Drosophila brain by magnetic resonance microscopy at 10 micron isotropic resolution. *Scientific Reports*, *5*, 8920.

34. Yu, X., He, Y., Wang, M., Merkle, H., Dodd, S. J., Silva, A. C., & Koretsky, A. P. (2016). Sensory and optogenetically driven single-vessel fMRI. *Nature Methods*, *13*(4), 337–340.

35. Yu, X., Qian, C., Chen, D., Dodd, S., & Koretsky, A. P. (2014). Deciphering laminar-specific neural inputs with line-scanning fMRI. *Nature Methods*, *11*(1), 55–58.

36. Lustig, M., Donoho, D., & Pauly, J. M. (2007). Sparse MRI: The application of compressed sensing for rapid MR imaging. *Magnetic Resonance in Medicine*, *58*(6), 1182–1195.

37. Larkman, D. J., Hajnal, J. V, Herlihy, A. H., Coutts, G. A., Young, I. R., & Ehnholm, G. (2001). Use of multicoil arrays for separation of signal from multiple slices simultaneously excited. *Journal of Magnetic Resonance Imaging : JMRI*, *13*(2), 313–317.

38. Budinger, T. F., & Bird, M. D. (2018). MRI and MRS of the human brain at magnetic fields of 14 T to 20 T: Technical feasibility, safety, and neuroscience horizons. *NeuroImage*, *168*, 509–531.

39. Lauffer, R. B. (1987). Paramagnetic metal complexes as water proton relaxation agents for NMR imaging: theory and design. *Chemical Reviews*, *87*(5), 901–927.

40. Weinmann, H., Brasch, R., Press, W., & Wesbey, G. (1984). Characteristics of gadolinium-DTPA complex: a potential NMR contrast agent. *American Journal of Roentgenology*, *142*(3), 619–624.

41. Carr, D. , Brown, J., Bydder, G. ., Weinmann, H.-J., Speck, U., Thomas, D. ., & Young, I. . (1984). INTRAVENOUS CHELATED GADOLINIUM AS A CONTRAST AGENT IN NMR IMAGING OF CEREBRAL TUMOURS. *The Lancet*, *323*(8375), 484–486.

42. Pierre, V. C., Allen, M. J., & Caravan, P. (2014). Contrast agents for MRI: 30+ years and where are we going? *Journal of Biological Inorganic Chemistry : JBIC : A Publication of the Society of Biological Inorganic Chemistry*, *19*(2), 127–131.

43. Kanda, T., Fukusato, T., Matsuda, M., Toyoda, K., Oba, H., Kotoku, J., ... Furui, S. (2015). Gadolinium-based Contrast Agent Accumulates in the Brain Even in Subjects without Severe Renal Dysfunction: Evaluation of Autopsy Brain Specimens with Inductively Coupled Plasma Mass Spectroscopy. *Radiology*, *276*(1), 228–232.

44. Kanal, E. (2016). Gadolinium based contrast agents (GBCA): Safety overview after 3 decades of clinical experience. *Magnetic Resonance Imaging*, *34*(10), 1341–1345.

45. Pan, D., Schmieder, A. H., Wickline, S. A., & Lanza, G. M. (2011). Manganese-based MRI contrast agents: past, present and future. *Tetrahedron*, *67*(44), 8431–8444.

46. Kanda, T., Fukusato, T., Matsuda, M., Toyoda, K., Oba, H., Kotoku, J., ... Furui, S. (2015). Gadolinium-based Contrast Agent Accumulates in the Brain Even in Subjects without Severe Renal Dysfunction: Evaluation of Autopsy Brain Specimens with Inductively Coupled Plasma Mass Spectroscopy. *Radiology*, *276*(1), 228–232.

47. Barandov, A., Bartelle, B. B., Gonzalez, B. A., White, W. L., Lippard, S. J., & Jasanoff, A. (2016). Membrane-Permeable Mn(III) Complexes for Molecular Magnetic Resonance Imaging of Intracellular Targets. *Journal of the American Chemical Society*, *138*(17), 5483–5486.

48. Skjold, A., Amundsen, B. H., Wiseth, R., Støylen, A., Haraldseth, O., Larsson, H. B. W., & Jynge, P. (2007). Manganese dipyridoxyl-diphosphate (MnDPDP) as a viability marker in patients with myocardial infarction. *Journal of Magnetic Resonance Imaging*, *26*(3), 720–727.

49. Lin, Y. J., & Koretsky, A. P. (1997). Manganese ion enhances T1-weighted MRI during brain activation: an approach to direct imaging of brain function. *Magnetic Resonance in Medicine*, *38*(3), 378–388.

50. Malheiros, J. M., Paiva, F. F., Longo, B. M., Hamani, C., & Covolan, L. (2015). Manganese-Enhanced MRI: Biological Applications in Neuroscience. *Frontiers in Neurology*, *6*, 161.

51. Perez, J. M., Josephson, L., O'Loughlin, T., Högemann, D., & Weissleder, R. (2002). Magnetic relaxation switches capable of sensing molecular interactions. *Nature Biotechnology*, *20*(8), 816–820.

52. Atanasijevic, T., Shusteff, M., Fam, P., & Jasanoff, A. (2006). Calcium-sensitive MRI contrast agents based on superparamagnetic iron oxide nanoparticles and calmodulin. *Proceedings of the National Academy of Sciences of the United States of America*, *103*(40), 14707–14712.

53. Okada, S., Bartelle, B. B., Li, N., Breton-Provencher, V., Lee, J. J., Rodriguez, E., ... Jasanoff, A. (2018). Calcium-dependent molecular fMRI using a magnetic nanosensor. *Nature Nanotechnology*, *13*(6), 473–477.

54. Louie, A. Y., Hüber, M. M., Ahrens, E. T., Rothbächer, U., Moats, R., Jacobs, R. E., ... Meade, T. J. (2000). In vivo visualization of gene expression using magnetic resonance imaging. *Nature Biotechnology*, *18*(3), 321–325.

55. Shapiro, M. G., Szablowski, J. O., Langer, R., & Jasanoff, A. (2009). Protein nanoparticles engineered to sense kinase activity in MRI. *Journal of the American Chemical Society*, *131*(7), 2484–2486.

56. Genove, G., DeMarco, U., Xu, H., Goins, W. F., & Ahrens, E. T. (2005). A new transgene reporter for in vivo magnetic resonance imaging. *Nature Medicine*, *11*(4), 450–454.

57. Cohen, B., Dafni, H., Meir, G., Harmelin, A., & Neeman, M. (2005). Ferritin as an Endogenous MRI Reporter for Noninvasive Imaging of Gene Expression in C6 Glioma Tumors. *Neoplasia (New York, N.Y.)*, *7*(2), 109–117.

58. Iordanova, B., Robison, C. S., & Ahrens, E. T. (2010). Design and characterization of a chimeric ferritin with enhanced iron loading and transverse NMR relaxation rate. *Journal of Biological Inorganic Chemistry : JBIC : A Publication of the Society of Biological Inorganic Chemistry*, *15*(6), 957–965.

59. Iordanova, B., Hitchens, T. K., Robison, C. S., & Ahrens, E. T. (2013). Engineered Mitochondrial Ferritin as a Magnetic Resonance Imaging Reporter in Mouse Olfactory Epithelium. *PLoS ONE*, *8*(8), e72720.

60. Matsumoto, Y., Chen, R., Anikeeva, P., & Jasanoff, A. (2015). Engineering intracellular biomineralization and biosensing by a magnetic protein. *Nature Communications*, *6*, 8721.

61. Bernau, K., Lewis, C. M., Petelinsek, A. M., Reagan, M. S., Niles, D. J., Mattis, V. B., ... Svendsen, C. N. (2016). In Vivo Tracking of Human Neural Progenitor Cells in the Rat Brain Using Magnetic Resonance Imaging Is Not Enhanced by Ferritin Expression. *Cell Transplantation*, *25*(3), 575–592.

62. Genove, G., DeMarco, U., Xu, H., Goins, W. F., & Ahrens, E. T. (2005). A new transgene reporter for in vivo magnetic resonance imaging. *Nature Medicine*, *11*(4), 450–454.

63. Bartelle, B. B., Szulc, K. U., Suero-Abreu, G. A., Rodriguez, J. J., & Turnbull, D. H. (2013). Divalent Metal Transporter, DMT1: A Novel MRI Reporter Protein. *Magnetic Resonance in Medicine : Official Journal of the Society of Magnetic Resonance in Medicine / Society of Magnetic Resonance in Medicine*, *70*(3), 842–850.

64. Schilling, F., Ros, S., Hu, D.-E., D'Santos, P., McGuire, S., Mair, R., ... Brindle, K. M. (2017). MRI measurements of reporter-mediated increases in transmembrane water exchange enable detection of a gene reporter. *Nature Biotechnology*, *35*(1), 75–80.

65. Mukherjee, A., Wu, D., Davis, H. C., & Shapiro, M. G. (2016). Non-invasive

imaging using reporter genes altering cellular water permeability. *Nature Communications*, *7*, 13891.

66. Shapiro, M. G., Westmeyer, G. G., Romero, P. A., Szablowski, J. O., Küster, B., Shah, A., ... Jasanoff, A. (2010). Directed evolution of a magnetic resonance imaging contrast agent for noninvasive imaging of dopamine. *Nature Biotechnology*, *28*(3), 264–270.

67. Lee, T., Cai, L. X., Lelyveld, V. S., Hai, A., & Jasanoff, A. (2014). Molecular-Level Functional Magnetic Resonance Imaging of Dopaminergic Signaling. *Science*, *344*(6183), 533–535.

68. Brustad, E. M., Lelyveld, V. S., Snow, C. D., Crook, N., Jung, S. T., Martinez, F. M., ... Arnold, F. H. (2012). Structure-Guided Directed Evolution of Highly Selective P450-based Magnetic Resonance Imaging Sensors for Dopamine and Serotonin. *Journal of Molecular Biology*, *422*(2), 245–262.

69. Hai, A., Cai, L. X., Lee, T., Lelyveld, V. S., & Jasanoff, A. (2016). Molecular fMRI of serotonin transport. *Neuron*, *92*(4), 754–765.

70. Busija, D. W., Bari, F., Domoki, F., & Louis, T. (2007). Mechanisms Involved in the Cerebrovascular Dilator Effects of N-methyl-D-aspartate in Cerebral Cortex. *Brain Research Reviews*, *56*(1), 89–100.

71. Lee, T., Cai, L. X., Lelyveld, V. S., Hai, A., & Jasanoff, A. (2014). Molecular-Level Functional Magnetic Resonance Imaging of Dopaminergic Signaling. *Science*, *344*(6183), 533–535.

72. Yang, G., Zhang, Y., Ross, M. E., & Iadecola, C. (2003). Attenuation of activity-induced increases in cerebellar blood flow in mice lacking neuronal nitric oxide synthase. *American Journal of Physiology-Heart and Circulatory Physiology*, *285*(1), H298–H304.

73. Ma, J., Ayata, C., Huang, P. L., Fishman, M. C., & Moskowitz, M. A. (1996). Regional cerebral blood flow response to vibrissal stimulation in mice lacking type I NOS gene expression. *American Journal of Physiology-Heart and Circulatory Physiology*, *270*(3), H1085–H1090.

74. Leithner, C., Royl, G., Offenhauser, N., Füchtemeier, M., Kohl-Bareis, M., Villringer, A., ... Lindauer, U. (2010). Pharmacological uncoupling of activation induced increases in CBF and $CMRO_2$. *Journal of Cerebral Blood Flow and Metabolism: Official Journal of the International Society of Cerebral Blood Flow and Metabolism*, *30*(2), 311–322.

75. Stefanovic, B., Schwindt, W., Hoehn, M., & Silva, A. C. (2007). Functional Uncoupling of Hemodynamic from Neuronal Response by Inhibition of Neuronal Nitric Oxide Synthase. *Journal of Cerebral Blood Flow & Metabolism*, *27*(4), 741–754.

76. Desai, M., Slusarczyk, A. L., Chapin, A., Barch, M., & Jasanoff, A. (2016). Molecular imaging with engineered physiology. *Nature Communications*, *7*, 13607.

77. Iderton, W. K., Cooper, C. E., & Knowles, R. G. (2001). Nitric oxide synthases: structure, function and inhibition. *Biochemical Journal*, *357*(Pt 3), 593–615.

78. Vallance, P., & Leiper, J. (2002). Blocking NO synthesis: how, where and why? *Nature Reviews Drug Discovery*, *1*(12), 939–950.

79. Fedorov, R., Vasan, R., Ghosh, D. K., & Schlichting, I. (2004). Structures of nitric oxide synthase isoforms complexed with the inhibitor AR-R17477 suggest a rational basis for specificity and inhibitor design. *Proceedings of the National Academy of Sciences of the United States of America*, *101*(16), 5892–5897.

80. Lee, S. J., & Stull, J. T. (1998). Calmodulin-dependent regulation of inducible and neuronal nitric-oxide synthase. *The Journal of Biological Chemistry*, *273*(42), 27430–27437.

81. Fang, J., & Silverman, R. B. (2009). A Cellular Model for Screening Neuronal Nitric Oxide Synthase Inhibitors. *Analytical Biochemistry*, *390*(1), 74–78.

82. Hendrie, P. C., & Russell, D. W. (2005). Gene targeting with viral vectors. *Molecular Therapy : The Journal of the American Society of Gene Therapy*, *12*(1), 9–17.

83. Hegemann, P., & Nagel, G. (2013). From channelrhodopsins to optogenetics. *EMBO Molecular Medicine*, *5*(2), 173–176.

84. Herlenius, E., & Lagercrantz, H. (2001). Neurotransmitters and neuromodulators during early human development. *Early Human Development*, *65*(1), 21–37.

85. Levin, E. D. (Ed.). (2006). *Neurotransmitter Interactions and Cognitive Function* (Vol. 98). Birkhäuser Basel.

86. Myhrer, T. (2003). Neurotransmitter systems involved in learning and memory in the rat: a meta-analysis based on studies of four behavioral tasks. *Brain Research Reviews*, *41*(2–3), 268–287.

87. Francis, P. T. (2005). The interplay of neurotransmitters in Alzheimer's disease. *CNS Spectrums*, *10*(11 Suppl 18), 6–9.

88. Cowen, P. J., & Browning, M. (2015). What has serotonin to do with depression? *World Psychiatry*, *14*(2), 158–160.

89. Baird, G. S., Zacharias, D. A., & Tsien, R. Y. (1999). Circular permutation and receptor insertion within green fluorescent proteins. *Proceedings of the National Academy of Sciences of the United States of America*, *96*(20), 11241–11246.

90. Rutter, G. A., Burnett, P., Rizzuto, R., Brini, M., Murgia, M., Pozzan, T., … Denton, R. M. (1996). Subcellular imaging of intramitochondrial Ca2+ with recombinant targeted aequorin: significance for the regulation of pyruvate dehydrogenase activity. *Proceedings of the National Academy of Sciences of the United States of America*, *93*(11), 5489–5494.

91. Marvin, J. S., Borghuis, B. G., Tian, L., Cichon, J., Harnett, M. T., Akerboom, J., … Looger, L. L. (2013). An optimized fluorescent probe for visualizing glutamate neurotransmission. *Nature Methods*, *10*(2), 162–170.

92. Rutter, G. A., Burnett, P., Rizzuto, R., Brini, M., Murgia, M., Pozzan, T., … Denton, R. M. (1996). Subcellular imaging of intramitochondrial Ca2+ with recombinant targeted aequorin: significance for the regulation of pyruvate dehydrogenase activity. *Proceedings of the National Academy of Sciences of the United States of America*, *93*(11), 5489–5494.

93. Patriarchi, T., Cho, J. R., Merten, K., Howe, M. W., Marley, A., Xiong, W.-H., … Tian, L. (2018). Ultrafast neuronal imaging of dopamine dynamics with designed genetically encoded sensors. *Science*, *360*(6396), eaat4422.

94. Sun, F., Zeng, J., Jing, M., Zhou, J., Feng, J., Owen, S. F., ... Li, Y. (2018). A Genetically Encoded Fluorescent Sensor Enables Rapid and Specific Detection of Dopamine in Flies, Fish, and Mice. *Cell*, *174*(2), 481–496.

95. Muller, A., Joseph, V., Slesinger, P. A., & Kleinfeld, D. (2014). Cell-based reporters reveal *in vivo* dynamics of dopamine and norepinephrine release in murine cortex. *Nature Methods*, *11*(12), 1245–1252.

96. Nguyen, Q.-T., Schroeder, L. F., Mank, M., Muller, A., Taylor, P., Griesbeck, O., & Kleinfeld, D. (2010). An *in vivo* biosensor for neurotransmitter release and *in situ* receptor activity. *Nature Neuroscience*, *13*(1), 127–132.

97. Gibson, D. G., Young, L., Chuang, R.-Y., Venter, J. C., Hutchison, C. A., & Smith, H. O. (2009). Enzymatic assembly of DNA molecules up to several hundred kilobases. *Nature Methods*, *6*(5), 343–345.

98. Okada, S., Bartelle, B. B., Li, N., Breton-Provencher, V., Lee, J. J., Rodriguez, E., ... Jasanoff, A. (2018). Calcium-dependent molecular fMRI using a magnetic nanosensor. *Nature Nanotechnology*, *13*(6), 473–477.

99. Grynkiewicz, G., Poenie, M., & Tsien, R. Y. (1985). A new generation of Ca2+ indicators with greatly improved fluorescence properties. *The Journal of Biological Chemistry*, *260*(6), 3440–3450.

100. Piascik, M. T., & Perez, D. M. (2001). Alpha1-adrenergic receptors: new insights and directions. *The Journal of Pharmacology and Experimental Therapeutics*, *298*(2), 403–410.

101. Jasanoff, A. (2007). Bloodless fMRI. *Trends in Neurosciences*, *30*(11), 603–610.

102. Shen, Z., Wu, A., & Chen, X. (2017). Iron Oxide Nanoparticle Based Contrast Agents for Magnetic Resonance Imaging. *Molecular Pharmaceutics*, *14*(5), 1352–1364.

103. Rodriguez, E., Lelyveld, V. S., Atanasijevic, T., Okada, S., & Jasanoff, A. (2014). Magnetic nanosensors optimized for rapid and reversible self-assembly. *Chemical Communications (Cambridge, England)*, *50*(27), 3595–3598.

104. Kim, H. S., Woo, J., Lee, J. H., Joo, H. J., Choi, Y., Kim, H., … Kim, S. J. (2015). In vivo Tracking of Dendritic Cell using MRI Reporter Gene, Ferritin. *PLOS ONE*, *10*(5), e0125291.

105. Ziv, K., Meir, G., Harmelin, A., Shimoni, E., Klein, E., & Neeman, M. (2010). Ferritin as a reporter gene for MRI: Chronic liver over expression of h-Ferritin during dietary iron supplementation and aging. *NMR in Biomedicine*, *23*(5), 523–531.

106. Pereira, S. M., Moss, D., Williams, S. R., Murray, P., & Taylor, A. (2015). Overexpression of the MRI Reporter Genes Ferritin and Transferrin Receptor Affect Iron Homeostasis and Produce Limited Contrast in Mesenchymal Stem Cells. *International Journal of Molecular Sciences*, *16*(7), 15481–15496.

107. O'Callaghan, D. W., Tepikin, A. V., & Burgoyne, R. D. (2003). Dynamics and calcium sensitivity of the Ca^{2+}/myristoyl switch protein hippocalcin in living cells. *The Journal of Cell Biology*, *163*(4), 715–721.

108. Baichoo, N., & Helmann, J. D. (2002). Recognition of DNA by Fur: a reinterpretation of the Fur box consensus sequence. *Journal of Bacteriology*, *184*(21), 5826–5832.

109. Baichoo, N., & Helmann, J. D. (2002). Recognition of DNA by Fur: a reinterpretation of the Fur box consensus sequence. *Journal of Bacteriology*, *184*(21), 5826–5832.

110. Tatur, J., Hagen, W. R., & Matias, P. M. (2007). Crystal structure of the ferritin from the hyperthermophilic archaeal anaerobe *Pyrococcus furiosus*. *Journal of Biological Inorganic Chemistry*, *12*(5), 615–630.

111. Stillman, T. ., Hempstead, P. ., Artymiuk, P. ., Andrews, S. ., Hudson, A. ., Treffry, A., ... Harrison, P. . (2001). The high-resolution X-ray crystallographic structure of the ferritin (EcFtnA) of Escherichia coli; comparison with human H ferritin (HuHF) and the structures of the Fe3+ and Zn2+. *Journal of Molecular Biology*, *307*(2), 587–603.

112. Johnson, E., Cascio, D., Sawaya, M. R., Gingery, M., & Schröder, I. (2005). Crystal Structures of a Tetrahedral Open Pore Ferritin from the Hyperthermophilic Archaeon Archaeoglobus fulgidus. *Structure*, *13*(4), 637–648.

113. Sana, B., Johnson, E., Sheah, K., Poh, C. L., & Lim, S. (2010). Iron-based ferritin nanocore as a contrast agent. *Biointerphases*, *5*(3), FA48-FA52.

114. Guan, L., Liu, Q., Li, C., & Zhang, Y. (2013). Development of a Fur-dependent and tightly regulated expression system in *Escherichia coli* for toxic protein synthesis. *BMC Biotechnology*, *13*, 25.

115. Rogers, T. B., Inesi, G., Wade, R., & Lederer, W. J. (1995). Use of thapsigargin to study Ca2+ homeostasis in cardiac cells. *Bioscience Reports*, *15*(5), 341–349.

116. Rouault, T. A. (2003). How Mammals Acquire and Distribute Iron Needed for Oxygen-Based Metabolism. *PLoS Biology*, *1*(3), e79.

117. Matsumoto, Y., & Jasanoff, A. (2008). T2 relaxation induced by clusters of superparamagnetic nanoparticles: Monte Carlo simulations. *Magnetic Resonance Imaging*, *26*(7), 994–998.

APPENDIX I

Coding sequences of constructs used in this thesis

i) Coding sequence for rat nNOS:

ATGGAAGAGAACACGTTTGGGGTTCAGCAGATCCAACCCAATGTAATTTCTG
TTCGTCTCTTCAAACGCAAAGTGGGAGGTCTGGGCTTCCTGGTGAAGGAACG
GGTCAGCAAGCCTCCCGTGATCATCTCAGACCTGATTCGAGGAGGTGCTGCG
GAGCAGAGCGGCCTTATCCAAGCTGGAGACATCATTCTCGCAGTCAACGATC
GGCCCTTGGTAGACCTCAGCTATGACAGTGCCCTGGAGGTTCTCAGGGGCAT
TGCCTCTGAGACCCACGTGGTCCTCATTCTGAGGGGCCCTGAGGGCTTCACTA
CACATCTGGAGACCACCTTCACAGGGGATGGAACCCCCAAGACCATCCGGGT
GACCCAGCCCCTCGGTCCTCCCACCAAAGCCGTCGATCTGTCTCACCAGCCTT
CAGCCAGCAAAGACCAGTCATTAGCAGTAGACAGAGTCACAGGTCTGGGTA
ATGGCCCTCAGCATGCCCAAGGCCATGGGCAGGGAGCTGGCTCAGTCTCCCA
AGCTAATGGTGTGGCCATTGACCCCACGATGAAAAGCACCAAGGCCAACCTC
CAGGACATCGGGGAACATGATGAACTGCTCAAAGAGATAGAACCTGTGCTG
AGCATCCTCAACAGTGGGAGCAAAGCCACCAACAGAGGGGGACCAGCCAAA
GCAGAGATGAAAGACACAGGAATCCAGGTGGACAGAGACCTCGATGGCAAA
TCGCACAAAGCTCCGCCCCTGGGCGGGGACAATGACCGCGTCTTCAATGACC
TGTGGGGGAAGGACAACGTTCCTGTGGTCCTTAACAACCCGTATTCAGAGAA
GGAACAGTCCCCTACCTCGGGGAAACAGTCTCCCACCAAGAACGGCAGCCCT
TCCAGGTGCCCCCGTTTCCTCAAGGTCAAGAACTGGGAGACGGACGTGGTCC
TCACCGACACCCTGCACCTGAAGAGCACACTGGAAACGGGGTGCACAGAGC
ACATTTGCATGGGCTCGATCATGCTGCCTTCCCAGCACACGCGGAAGCCAGA
AGATGTCCGCACAAAGGACCAGCTCTTCCCTCTAGCCAAAGAATTTCTCGAC
CAATACTACTCATCCATTAAGAGATTTGGCTCCAAGGCCCACATGGACAGGC
TGGAGGAGGTGAACAAGGAGATTGAAAGCACCAGCACCTACCAGCTCAAGG
ACACCGAGCTCATCTATGGCGCCAAGCATGCCTGGCGGAACGCCTCTCGATG
TGTGGGCAGGATCCAGTGGTCCAAGCTGCAGGTGTTCGATGCCCGAGACTGC
ACCACAGCCCACGGCATGTTCAACTACATCTGTAACCATGTCAAGTATGCCA
CCAACAAAGGGAATCTCAGGTCGGCCATCACGATATTCCCTCAGAGGACTGA
CGGCAAACATGACTTCCGAGTGTGGAACTCGCAGCTCATCCGCTACGCGGGC
TACAAGCAGCCAGATGGCTCTACCTTGGGGGATCCAGCCAATGTGCAGTTCA
CGGAGATCTGTATACAGCAGGGCTGGAAAGCCCCAAGAGGCCGCTTCGACGT
GCTGCCTCTCCTGCTTCAGGCCAATGGCAATGACCCTGAGCTCTTCCAGATCC
CCCCAGAGCTGGTGCTGGAAGTGCCCATCAGGCACCCCAAGTTCGACTGGTT
TAAGGACCTGGGGCTCAAATGGTATGGCCTCCCCGCTGTGTCCAACATGCTG
CTGGAGATCGGGGGCCTGGAGTTCAGCGCCTGTCCCTTCAGCGGCTGGTACA
TGGGCACAGAGATCGGCGTCCGTGACTACTGTGACAACTCTCGATACAACAT
CCTGGAGGAAGTAGCCAAGAAGATGGATTTGGACATGAGGAAGACCTCGTC
CCTCTGGAAGGACCAAGCACTGGTGGAGATCAACATTGCTGTTCTATATAGC
TTCCAGAGTGACAAGGTGACCATCGTTGACCACCACTCTGCCACGGAGTCCT
TCATCAAACACATGGAGAATGAATACCGCTGCAGAGGGGGCTGCCCCGCCGA
CTGGGTGTGGATTGTGCCTCCCATGTCGGGCAGCATCACCCCTGTCTTCCACC
AGGAGATGCTCAACTATAGACTCACCCCGTCCTTTGAATACCAGCCTGATCC

ATGGAACACCCACGTGTGGAAGGGCACCAACGGGACCCCCACGAAGCGGCG
AGCTATCGGCTTTAAGAAATTGGCAGAGGCCGTCAAGTTCTCAGCCAAGCTA
ATGGGGCAGGCCATGGCCAAGAGGGTCAAGGCGACCATTCTCTACGCCACAG
AGACAGGCAAATCACAAGCCTATGCCAAGACCCTGTGTGAGATCTTCAAGCA
CGCCTTCGATGCCAAGGCAATGTCCATGGAGGAGTATGACATCGTGCACCTG
GAGCACGAAGCCCTGGTCTTGGTGGTCACCAGCACCTTTGGCAATGGAGACC
CCCCTGAGAACGGGGAGAAATTCGGCTGTGCTTTAATGGAGATGAGGCACCC
CAACTCTGTGCAGGAGGAGAGAAAGAGCTACAAGGTCCGATTCAACAGCGT
CTCCTCCTATTCTGACTCCCGAAAGTCATCGGGCGACGGACCCGACCTCAGA
GACAACTTTGAAAGTACTGGACCCCTGGCCAATGTGAGGTTCTCAGTGTTCG
GCCTCGGCTCTCGGGCGTACCCCCACTTCTGTGCCTTTGGGCATGCGGTGGAC
ACCCTCCTGGAGGAACTGGGAGGGGAGAGGATTCTGAAGATGAGGGAGGGG
GATGAGCTTTGCGGACAGGAAGAAGCTTTCAGGACCTGGGCCAAGAAAGTCT
TCAAGGCAGCCTGTGATGTGTTCTGCGTGGGGGATGACGTCAACATCGAGAA
GGCGAACAACTCCCTCATTAGCAATGACCGAAGCTGGAAGAGGAACAAGTTC
CGCCTCACGTATGTGGCGGAAGCTCCAGATCTGACCCAAGGTCTTTCCAATGT
TCACAAAAAACGAGTCTCGGCTGCTCGACTCCTCAGCCGCCAAAACCTGCAA
AGCCCTAAGTCCAGCCGATCGACCATCTTCGTGCGTCTCCACACCAACGGGA
ATCAGGAGCTGCAGTACCAGCCAGGGGACCACCTGGGTGTCTTCCCCGGCAA
CCACGAGGACCTCGTGAATGCACTCATTGAACGGCTGGAGGATGCACCGCCT
GCCAACCACGTGGTGAAGGTGGAGATGCTGGAGGAGAGGAACACTGCTCTG
GGTGTCATCAGTAATTGGAAGGATGAATCTCGCCTCCCACCCTGCACCATCTT
CCAGGCCTTCAAGTACTACCTGGACATCACCACGCCGCCCACGCCCCTGCAG
CTGCAGCAGTTCGCCTCTCTGGCCACTAATGAGAAAGAGAAGCAGCGGTTGC
TGGTCCTCAGCAAGGGGCTCCAGGAATATGAGGAGTGGAAGTGGGGCAAGA
ACCCCACAATGGTGGAGGTGCTGGAGGAGTTCCCGTCCATCCAGATGCCGGC
TACACTTCTCCTCACTCAGCTGTCGCTGCTGCAGCCTCGCTACTACTCCATCA
GCTCCTCTCCAGACATGTACCCCGACGAGGTGCACCTCACTGTGGCCATCGTC
TCCTACCACACCCGAGACGGAGAAGGACCAGTCCACCACGGGGTGTGCTCCT
CCTGGCTCAACAGAATACAGGCTGACGATGTAGTCCCCTGCTTCGTGAGAGG
TGCCCCTAGCTTCCACCTGCCTCGAAACCCCCAGGTGCCTTGCATCCTGGTTG
GCCCAGGCACTGGCATCGCACCCTTCCGAAGCTTCTGGCAACAGCGACAATT
TGACATCCAACACAAAGGAATGAATCCGTGCCCCATGGTTCTGGTCTTCGGG
TGTCGACAATCCAAGATAGATCATATCTACAGAGAGGAGACCCTGCAGGCCA
AGAACAAGGGCGTCTTCAGAGAGCTGTACACTGCCTATTCCCGGGAACCGGA
CAGGCCAAAGAAATATGTACAGGACGTGCTGCAGGAACAGCTGGCTGAGTCT
GTGTACCGCGCCCTGAAGGAGCAAGGAGGCCACATTTATGTCTGTGGGGACG
TTACCATGGCCGCCGATGTCCTCAAAGCCATCCAGCGCATAATGACCCAGCA
GGGGAAACTCTCAGAGGAGGACGCTGGTGTATTCATCAGCAGGCTGAGGGAT
GACAACCGGTACCACGAGGACATCTTTGGAGTCACCCTCAGAACGTATGAAG
TGACCAACCGCCTTAGATCTGAGTCCATCGCCTTCATCGAAGAGAGCAAAAA
AGACGCAGATGAGGTTTTCAGCTCCTAA

ii) coding sequence for human iNOS:
ATGGCTTGTCCTTGGAAATTTCTGTTCAAGACCAAATTCCACCAGTATGCAAT
GAATGGGGAAAAAGACATCAACAACAATGTGGAGAAAGCCCCCTGTGCCAC

CTCCAGTCCAGTGACACAGGATGACCTTCAGTATCACAACCTCAGCAAGCAG
CAGAATGAGTCCCCGCAGCCCCTCGTGGAGACGGGAAAGAAGTCTCCAGAAT
CTCTGGTCAAGCTGGATGCAACCCCATTGTCCTCCCCACGGCATGTGAGGATC
AAAAACTGGGGCAGCGGGATGACTTTCCAAGACACACTTCACCATAAGGCCA
AAGGGATTTTAACTTGCAGGTCCAAATCTTGCCTGGGGTCCATTATGACTCCC
AAAAGTTTGACCAGAGGACCCAGGGACAAGCCTACCCCTCCAGATGAGCTTC
TACCTCAAGCTATCGAATTTGTCAACCAATATTACGGCTCCTTCAAAGAGGCA
AAAATAGAGGAACATCTGGCCAGGGTGGAAGCGGTAACAAAGGAGATAGAA
ACAACAGGAACCTACCAACTGACGGGAGATGAGCTCATCTTCGCCACCAAGC
AGGCCTGGCGCAATGCCCCACGCTGCATTGGGAGGATCCAGTGGTCCAACCT
GCAGGTCTTCGATGCCCGCAGCTGTTCCACTGCCCGGGAAATGTTTGAACAC
ATCTGCAGACACGTGCGTTACTCCACCAACAATGGCAACATCAGGTCGGCCA
TCACCGTGTTCCCCCAGCGGAGTGATGGCAAGCACGACTTCCGGGTGTGGAA
TGCTCAGCTCATCCGCTATGCTGGCTACCAGATGCCAGATGGCAGCATCAGA
GGGGACCCTGCCAACGTGGAATTCACTCAGCTGTGCATCGACCTGGGCTGGA
AGCCCAAGTACGGCCGCTTCGATGTGGTCCCCCTGGTCCTGCAGGCCAATGG
CCGTGACCCTGAGCTCTTCGAAATCCCACCTGACCTTGTGCTTGAGGTGGCCA
TGGAACATCCCAAATACGAGTGGTTTCGGGAACTGGAGCTAAAGTGGTACGC
CCTGCCTGCAGTGGCCAACATGCTGCTTGAGGTGGGCGGCCTGGAGTTCCCA
GGGTGCCCCTTCAATGGCTGGTACATGGGCACAGAGATCGGAGTCCGGGACT
TCTGTGACGTCCAGCGCTACAACATCCTGGAGGAAGTGGGCAGGAGAATGGG
CCTGGAAACGCACAAGCTGGCCTCGCTCTGGAAAGACCAGGCTGTCGTTGAG
ATCAACATTGCTGTGCTCCATAGTTTCCAGAAGCAGAATGTGACCATCATGG
ACCACCACTCGGCTGCAGAATCCTTCATGAAGTACATGCAGAATGAATACCG
GTCCCGTGGGGGCTGCCCGGCAGACTGGATTTGGCTGGTCCCTCCCATGTCTG
GGAGCATCACCCCCGTGTTTCACCAGGAGATGCTGAACTACGTCCTGTCCCCT
TTCTACTACTATCAGGTAGAGGCCTGGAAAACCCATGTCTGGCAGGACGAGA
AGCGGAGACCCAAGAGAAGAGAGATTCCATTGAAAGTCTTGGTCAAAGCTGT
GCTCTTTGCCTGTATGCTGATGCGCAAGACAATGGCGTCCCGAGTCAGAGTC
ACCATCCTCTTTGCGACAGAGACAGGAAAATCAGAGGCGCTGGCCTGGGACC
TGGGGGCCTTATTCAGCTGTGCCTTCAACCCCAAGGTTGTCTGCATGGATAAG
TACAGGCTGAGCTGCCTGGAGGAGGAACGGCTGCTGTTGGTGGTGACCAGTA
CGTTTGGCAATGGAGACTGCCCTGGCAATGGAGAGAAACTGAAGAAATCGCT
CTTCATGCTGAAAGAGCTCAACAACAAATTCAGGTACGCTGTGTTTGGCCTC
GGCTCCAGCATGTACCCTCGGTTCTGCGCCTTTGCTCATGACATTGATCAGAA
GCTGTCCCACCTGGGGGCCTCTCAGCTCACCCCGATGGGAGAAGGGGATGAG
CTCAGTGGGCAGGAGGACGCCTTCCGCAGCTGGGCCGTGCAAACCTTCAAGG
CAGCCTGTGAGACGTTTGATGTCCGAGGCAAACAGCACATTCAGATCCCCAA
GCTCTACACCTCCAATGTGACCTGGGACCCGCACCACTACAGGCTCGTGCAG
GACTCACAGCCTTTGGACCTCAGCAAAGCCCTCAGCAGCATGCATGCCAAGA
ACGTGTTCACCATGAGGCTCAAATCTCGGCAGAATCTACAAAGTCCGACATC
CAGCCGTGCCACCATCCTGGTGGAACTCTCCTGTGAGGATGGCCAAGGCCTG
AACTACCTGCCGGGGGAGCACCTTGGGGTTTGCCCAGGCAACCAGCCGGCCC
TGGTCCAAGGCATCCTGGAGCGAGTGGTGGATGGCCCCACACCCCACCAGAC
AGTGCGCCTGGAGGCCCTGGATGAGAGTGGCAGCTACTGGGTCAGTGACAAG
AGGCTGCCCCCCTGCTCACTCAGCCAGGCCCTCACCTACTTCCTGGACATCAC

CACACCCCCAACCCAGCTGCTGCTCCAAAAGCTGGCCCAGGTGGCCACAGAA
GAGCCTGAGAGACAGAGGCTGGAGGCCCTGTGCCAGCCCTCAGAGTACAGC
AAGTGGAAGTTCACCAACAGCCCCACATTCCTGGAGGTGCTAGAGGAGTTCC
CGTCCCTGCGGGTGTCTGCTGGCTTCCTGCTTTCCCAGCTCCCCATTCTGAAG
CCCAGCTTCTACTCCATCAGCTCCTCCCGGGATCACACGCCCACGGAGATCCA
CCTGACTGTGGCCGTGGTCACCTACCACACCCGAGATGGCCAGGGTCCCCTG
CACCACGGCGTCTGCAGCACATGGCTCAACAGCCTGAAGCCCCAAGACCCAG
TGCCCTGCTTTGTGCGGAATGCCAGCGGCTTCCACCTCCCCGAGGATCCCTCC
CATCCTTGCATCCTCATCGGGCCTGGCACAGGCATCGCGCCCTTCCGCAGTTT
CTGGCAGCAACGGCTCCATGACTCCCAGCACAAGGGAGTGCGGGGAGGCCG
CATGACCTTGGTGTTTGGGTGCCGCCGCCCAGATGAGGACCACATCTACCAG
GAGGAGATGCTGGAGATGGCCCAGAAGGGGGTGCTGCATGCGGTGCACACA
GCCTATTCCCGCCTGCCTGGCAAGCCCAAGGTCTATGTTCAGGACATCCTGCG
GCAGCAGCTGGCCAGCGAGGTGCTCCGTGTGCTCCACAAGGAGCCAGGCCAC
CTCTATGTTTGCGGGGATGTGCGCATGGCCCGGGACGTGGCCCACACCCTGA
AGCAGCTGGTGGCTGCCAAGCTGAAATTGAATGAGGAGCAGGTCGAGGACT
ATTTCTTTCAGCTCAAGAGCCAGAAGCGCTATCACGAAGATATCTTTGGTGCT
GTATTTCCTTACGAGGCGAAGAAGGACAGGGTGGCGGTGCAGCCCAGCAGCC
TGGAGATGTCAGCGCTCTGA

iii) coding sequence of NOSTIC-1
ATGGCTTGTCCTTGGAAATTTCTGTTCAAGACCAAATTCCACCAGTATGCAAT
GAATGGGGAAAAAGACATCAACAACAATGTGGAGAAAGCCCCCTGTGCCAC
CTCCAGTCCAGTGACACAGGATGACCTTCAGTATCACAACCTCAGCAAGCAG
CAGAATGAGTCCCCGCAGCCCCTCGTGGAGACGGGAAAGAAGTCTCCAGAAT
CTCTGGTCAAGCTGGATGCAACCCCATTGTCCTCCCCACGGCATGTGAGGATC
AAAAACTGGGGCAGCGGGATGACTTTCCAAGACACACTTCACCATAAGGCCA
AAGGGATTTTAACTTGCAGGTCCAAATCTTGCCTGGGGTCCATTATGACTCCC
AAAAGTTTGACCAGAGGACCCAGGGACAAGCCTACCCCTCCAGATGAGCTTC
TACCTCAAGCTATCGAATTTGTCAACCAATATTACGGCTCCTTCAAAGAGGCA
AAAATAGAGGAACATCTGGCCAGGGTGGAAGCGGTAACAAAGGAGATAGAA
ACAACAGGAACCTACCAACTGACGGGAGATGAGCTCATCTTCGCCACCAAGC
AGGCCTGGCGCAATGCCCCACGCTGCATTGGGAGGATCCAGTGGTCCAACCT
GCAGGTCTTCGATGCCCGCAGCTGTTCCACTGCCCGGGAAATGTTTGAACAC
ATCTGCAGACACGTGCGTTACTCCACCAACAATGGCAACATCAGGTCGGCCA
TCACCGTGTTCCCCCAGCGGAGTGATGGCAAGCACGACTTCCGGGTGTGGAA
TGCTCAGCTCATCCGCTATGCTGGCTACCAGATGCCAGATGGCAGCATCAGA
GGGGACCCTGCCAACGTGGAATTCACTCAGCTGTGCATCGACCTGGGCTGGA
AGCCCAAGTACGGCCGCTTCGATGTGGTCCCCCTGGTCCTGCAGGCCAATGG
CCGTGACCCTGAGCTCTTCGAAATCCCACCTGACCTTGTGCTTGAGGTGGCCA
TGGAACATCCCAAATACGAGTGGTTTCGGGAACTGGAGCTAAAGTGGTACGC
CCTGCCTGCAGTGGCCAACATGCTGCTTGAGGTGGGCGGCCTGGAGTTCCCA
GGGTGCCCCTTCAATGGCTGGTACATGGGCACAGAGATCGGAGTCCGGGACT
TCTGTGACGTCCAGCGCTACAACATCCTGGAGGAAGTGGGCAGGAGAATGGG
CCTGGAAACGCACAAGCTGGCCTCGCTCTGGAAAGACCAGGCTGTCGTTGAG
ATCAACATTGCTGTGCTCCATAGTTTCCAGAAGCAGAATGTGACCATCATGG

ACCACCACTCGGCTGCAGAATCCTTCATGAAGTACATGCAGAATGAATACCG
GTCCCGTGGGGGCTGCCCGGCAGACTGGATTTGGCTGGTCCCTCCCATGTCTG
GGAGCATCACCCCCGTGTTTCACCAGGAGATGCTGAACTACGTCCTGTCCCCT
TTCTACTACTATCAGGTAGAGGCCTGGAAAACCCATGTCTTTGAATACCAGCC
TGATCCATGGAACACCCACGTGTGGAAGGGCACCAACGGGACCCCCACGAA
GCGGCGAGCTATCGGCTTTAAGAAATTGGCAGAGGCCGTCAAGTTCTCAGCC
AAGCTAATGGGGCAGGCCATGGCCAAGAGGGTCAAGGCGACCATTCTCTACG
CCACAGAGACAGGCAAATCACAAGCCTATGCCAAGACCCTGTGTGAGATCTT
CAAGCACGCCTTCGATGCCAAGGCAATGTCCATGGAGGAGTATGACATCGTG
CACCTGGAGCACGAAGCCCTGGTCTTGGTGGTCACCAGCACCTTTGGCAATG
GAGACCCCCCTGAGAACGGGGAGAAATTCGGCTGTGCTTTAATGGAGATGAG
GCACCCCAACTCTGTGCAGGAGGAGAGAAAGAGCTACAAGGTCCGATTCAA
CAGCGTCTCCTCCTATTCTGACTCCCGAAAGTCATCGGGCGACGGACCCGAC
CTCAGAGACAACTTTGAAAGTACTGGACCCCTGGCCAATGTGAGGTTCTCAG
TGTTCGGCCTCGGCTCTCGGGCGTACCCCCACTTCTGTGCCTTTGGGCATGCG
GTGGACACCCTCCTGGAGGAACTGGGAGGGGAGAGGATTCTGAAGATGAGG
GAGGGGGATGAGCTTTGCGGACAGGAAGAAGCTTTCAGGACCTGGGCCAAG
AAAGTCTTCAAGGCAGCCTGTGATGTGTTCTGCGTGGGGGATGACGTCAACA
TCGAGAAGGCGAACAACTCCCTCATTAGCAATGACCGAAGCTGGAAGAGGA
ACAAGTTCCGCCTCACGTATGTGGCGGAAGCTCCAGATCTGACCCAAGGTCT
TTCCAATGTTCACAAAAAACGAGTCTCGGCTGCTCGACTCCTCAGCCGCCAA
AACCTGCAAAGCCCTAAGTCCAGCCGATCGACCATCTTCGTGCGTCTCCACA
CCAACGGGAATCAGGAGCTGCAGTACCAGCCAGGGGACCACCTGGGTGTCTT
CCCCGGCAACCACGAGGACCTCGTGAATGCACTCATTGAACGGCTGGAGGAT
GCACCGCCTGCCAACCACGTGGTGAAGGTGGAGATGCTGGAGGAGAGGAAC
ACTGCTCTGGGTGTCATCAGTAATTGGAAGGATGAATCTCGCCTCCCACCCTG
CACCATCTTCCAGGCCTTCAAGTACTACCTGGACATCACCACGCCGCCCACGC
CCCTGCAGCTGCAGCAGTTCGCCTCTCTGGCCACTAATGAGAAAGAGAAGCA
GCGGTTGCTGGTCCTCAGCAAGGGGCTCCAGGAATATGAGGAGTGGAAGTGG
GGCAAGAACCCCACAATGGTGGAGGTGCTGGAGGAGTTCCCGTCCATCCAGA
TGCCGGCTACACTTCTCCTCACTCAGCTGTCGCTGCTGCAGCCTCGCTACTAC
TCCATCAGCTCCTCTCCAGACATGTACCCCGACGAGGTGCACCTCACTGTGGC
CATCGTCTCCTACCACACCCGAGACGGAGAAGGACCAGTCCACCACGGGGTG
TGCTCCTCCTGGCTCAACAGAATACAGGCTGACGATGTAGTCCCCTGCTTCGT
GAGAGGTGCCCCTAGCTTCCACCTGCCTCGAAACCCCCAGGTGCCTTGCATCC
TGGTTGGCCCAGGCACTGGCATCGCACCCTTCCGAAGCTTCTGGCAACAGCG
ACAATTTGACATCCAACACAAAGGAATGAATCCGTGCCCCATGGTTCTGGTC
TTCGGGTGTCGACAATCCAAGATAGATCATATCTACAGAGAGGAGACCCTGC
AGGCCAAGAACAAGGGCGTCTTCAGAGAGCTGTACACTGCCTATTCCCGGGA
ACCGGACAGGCCAAAGAAATATGTACAGGACGTGCTGCAGGAACAGCTGGC
TGAGTCTGTGTACCGCGCCCTGAAGGAGCAAGGAGGCCACATTTATGTCTGT
GGGGACGTTACCATGGCCGCCGATGTCCTCAAAGCCATCCAGCGCATAATGA
CCCAGCAGGGGAAACTCTCAGAGGAGGACGCTGGTGTATTCATCAGCAGGCT
GAGGGATGACAACCGGTACCACGAGGACATCTTTGGAGTCACCCTCAGAACG
TATGAAGTGACCAACCGCCTTAGATCTGAGTCCATCGCCTTCATCGAAGAGA
GCAAAAAAGACGCAGATGAGGTTTTCAGCTCCTAA

iv) coding sequence of NOSTIC-2 with N-terminal His6 tag and C-terminal FLAG tag:
ATGCATCATCACCATCACCATATGGCTTGTCCTTGGAAATTTCTGTTCAAGAC
CAAATTCCACCAGTATGCAATGAATGGGGAAAAAGACATCAACAACAATGT
GGAGAAAGCCCCCTGTGCCACCTCCAGTCCAGTGACACAGGATGACCTTCAG
TATCACAACCTCAGCAAGCAGCAGAATGAGTCCCCGCAGCCCCTCGTGGAGA
CGGGAAAGAAGTCTCCAGAATCTCTGGTCAAGCTGGATGCAACCCCATTGTC
CTCCCCACGGCATGTGAGGATCAAAAACTGGGGCAGCGGGATGACTTTCCAA
GACACACTTCACCATAAGGCCAAAGGGATTTTAACTTGCAGGTCCAAATCTT
GCCTGGGGTCCATTATGACTCCCAAAAGTTTGACCAGAGGACCCAGGGACAA
GCCTACCCCTCCAGATGAGCTTCTACCTCAAGCTATCGAATTTGTCAACCAAT
ATTACGGCTCCTTCAAAGAGGCAAAAATAGAGGAACATCTGGCCAGGGTGG
AAGCGGTAACAAAGGAGATAGAAACAACAGGAACCTACCAACTGACGGGAG
ATGAGCTCATCTTCGCCACCAAGCAGGCCTGGCGCAATGCCCCACGCTGCAT
TGGGAGGATCCAGTGGTCCAACCTGCAGGTCTTCGATGCCCGCAGCTGTTCC
ACTGCCCGGGAAATGTTTGAACACATCTGCAGACACGTGCGTTACTCCACCA
ACAATGGCAACATCAGGTCGGCCATCACCGTGTTCCCCCAGCGGAGTGATGG
CAAGCACGACTTCCGGGTGTGGAATGCTCAGCTCATCCGCTATGCTGGCTAC
CAGATGCCAGATGGCAGCATCAGAGGGGACCCTGCCAACGTGGAATTCACTC
AGCTGTGCATCGACCTGGGCTGGAAGCCCAAGTACGGCCGCTTCGATGTGGT
CCCCCTGGTCCTGCAGGCCAATGGCCGTGACCCTGAGCTCTTCGAAATCCCAC
CTGACCTTGTGCTTGAGGTGGCCATGGAACATCCCAAATACGAGTGGTTTCG
GGAACTGGAGCTAAAGTGGTACGCCCTGCCTGCAGTGGCCAACATGCTGCTT
GAGGTGGGCGGCCTGGAGTTCCCAGGGTGCCCCTTCAATGGCTGGTACATGG
GCACAGAGATCGGAGTCCGGGACTTCTGTGACGTCCAGCGCTACAACATCCT
GGAGGAAGTGGGCAGGAGAATGGGCCTGGAAACGCACAAGCTGGCCTCGCT
CTGGAAAGACCAGGCTGTCGTTGAGATCAACATTGCTGTGCTCCATAGTTTCC
AGAAGCAGAATGTGACCATCATGGACCACCACTCGGCTGCAGAATCCTTCAT
GAAGTACATGCAGAATGAATACCGGTCCCGTGGGGGCTGCCCGGCAGACTGG
ATTTGGCTGGTCCCTCCCATGTCTGGGAGCATCACCCCCGTGTTTCACCAGGA
GATGCTGAACTACGTCCTGTCCCCTTTCTACTACTATCAGGTAGAGGCCTGGA
AAACCCATGTCTGGCAGGACGAGCCCACGAAGCGGCGAGCTATCGGCTTTAA
GAAATTGGCAGAGGCCGTCAAGTTCTCAGCCAAGCTAATGGGGCAGGCCATG
GCCAAGAGGGTCAAGGCGACCATTCTCTACGCCACAGAGACAGGCAAATCA
CAAGCCTATGCCAAGACCCTGTGTGAGATCTTCAAGCACGCCTTCGATGCCA
AGGCAATGTCCATGGAGGAGTATGACATCGTGCACCTGGAGCACGAAGCCCT
GGTCTTGGTGGTCACCAGCACCTTTGGCAATGGAGACCCCCCTGAGAACGGG
GAGAAATTCGGCTGTGCTTTAATGGAGATGAGGCACCCCAACTCTGTGCAGG
AGGAGAGAAAGAGCTACAAGGTCCGATTCAACAGCGTCTCCTCCTATTCTGA
CTCCCGAAAGTCATCGGGCGACGGACCCGACCTCAGAGACAACTTTGAAAGT
ACTGGACCCCTGGCCAATGTGAGGTTCTCAGTGTTCGGCCTCGGCTCTCGGGC
GTACCCCCACTTCTGTGCCTTTGGGCATGCGGTGGACACCCTCCTGGAGGAAC
TGGGAGGGGAGAGGATTCTGAAGATGAGGGAGGGGGATGAGCTTTGCGGAC

AGGAAGAAGCTTTCAGGACCTGGGCCAAGAAAGTCTTCAAGGCAGCCTGTGA
TGTGTTCTGCGTGGGGGATGACGTCAACATCGAGAAGGCGAACAACTCCCTC
ATTAGCAATGACCGAAGCTGGAAGAGGAACAAGTTCCGCCTCACGTATGTGG
CGGAAGCTCCAGATCTGACCCAAGGTCTTTCCAATGTTCACAAAAAACGAGT
CTCGGCTGCTCGACTCCTCAGCCGCCAAAACCTGCAAAGCCCTAAGTCCAGC
CGATCGACCATCTTCGTGCGTCTCCACACCAACGGGAATCAGGAGCTGCAGT
ACCAGCCAGGGGACCACCTGGGTGTCTTCCCCGGCAACCACGAGGACCTCGT
GAATGCACTCATTGAACGGCTGGAGGATGCACCGCCTGCCAACCACGTGGTG
AAGGTGGAGATGCTGGAGGAGAGGAACACTGCTCTGGGTGTCATCAGTAATT
GGAAGGATGAATCTCGCCTCCCACCCTGCACCATCTTCCAGGCCTTCAAGTAC
TACCTGGACATCACCACGCCGCCCACGCCCCTGCAGCTGCAGCAGTTCGCCT
CTCTGGCCACTAATGAGAAAGAGAAGCAGCGGTTGCTGGTCCTCAGCAAGGG
GCTCCAGGAATATGAGGAGTGGAAGTGGGGCAAGAACCCCACAATGGTGGA
GGTGCTGGAGGAGTTCCCGTCCATCCAGATGCCGGCTACACTTCTCCTCACTC
AGCTGTCGCTGCTGCAGCCTCGCTACTACTCCATCAGCTCCTCTCCAGACATG
TACCCCGACGAGGTGCACCTCACTGTGGCCATCGTCTCCTACCACACCCGAG
ACGGAGAAGGACCAGTCCACCACGGGGTGTGCTCCTCCTGGCTCAACAGAAT
ACAGGCTGACGATGTAGTCCCCTGCTTCGTGAGAGGTGCCCCTAGCTTCCACC
TGCCTCGAAACCCCCAGGTGCCTTGCATCCTGGTTGGCCCAGGCACTGGCATC
GCACCCTTCCGAAGCTTCTGGCAACAGCGACAATTTGACATCCAACACAAAG
GAATGAATCCGTGCCCCATGGTTCTGGTCTTCGGGTGTCGACAATCCAAGAT
AGATCATATCTACAGAGAGGAGACCCTGCAGGCCAAGAACAAGGGCGTCTTC
AGAGAGCTGTACACTGCCTATTCCCGGGAACCGGACAGGCCAAAGAAATATG
TACAGGACGTGCTGCAGGAACAGCTGGCTGAGTCTGTGTACCGCGCCCTGAA
GGAGCAAGGAGGCCACATTTATGTCTGTGGGGACGTTACCATGGCCGCCGAT
GTCCTCAAAGCCATCCAGCGCATAATGACCCAGCAGGGGAAACTCTCAGAGG
AGGACGCTGGTGTATTCATCAGCAGGCTGAGGGATGACAACCGGTACCACGA
GGACATCTTTGGAGTCACCCTCAGAACGTATGAAGTGACCAACCGCCTTAGA
TCTGAGTCCATCGCCTTCATCGAAGAGAGCAAAAAAGACGCAGATGAGGTTT
TCAGCTCCGGATCTGATTACAAAGACGACGACGACAAGTAA

v) coding sequence of PDZ-NOSTIC-2 with N-terminal His6 tag:
ATGCATCATCACCATCACCATATGGAAGAGAACACGTTTGGGGTTCAGCAGA
TCCAACCCAATGTAATTTCTGTTCGTCTCTTCAAACGCAAAGTGGGAGGTCTG
GGCTTCCTGGTGAAGGAACGGGTCAGCAAGCCTCCCGTGATCATCTCAGACC
TGATTCGAGGAGGTGCTGCGGAGCAGAGCGGCCTTATCCAAGCTGGAGACAT
CATTCTCGCAGTCAACGATCGGCCCTTGGTAGACCTCAGCTATGACAGTGCCC
TGGAGGTTCTCAGGGGCATTGCCTCTGAGACCCACGTGGTCCTCATTCTGAGG
GGCCCTGAGGGCTTCACTACACATCTGGAGACCACCTTCACAGGGGATGGAA
CCCCCAAGACCATCCGGGTGACCCAGCCCCTCGGTCCTCCCACCAAAGCCGT
CGATCTGTCTCACCAGCCTTCAGCCAGCAAAGACCAGTCATTAGCAGTAGAC
AGAGTCACAGGTCTGGGTAATGGCCCTCAGCATGCCCAAGGCCATGGGCAGG
GAGCTGGCTCAGTCTCCCAAGCTAATGGTGTGGCCATTGACCCCACGATGAA
AAGCACCAAGGCCAACCTCCAGGACATCGGGGAACATGATGAACTGCTCAA
AGAGATAGAACCTGTGCTGAGCATCCTCAACAGTGGGAGCAAAGCCACCAA
CAGAGGGGGACCAGCCAAAGCAGCTTGTCCTTGGAAATTTCTGTTCAAGACC

AAATTCCACCAGTATGCAATGAATGGGGAAAAAGACATCAACAACAATGTG
GAGAAAGCCCCCTGTGCCACCTCCAGTCCAGTGACACAGGATGACCTTCAGT
ATCACAACCTCAGCAAGCAGCAGAATGAGTCCCCGCAGCCCCTCGTGGAGAC
GGGAAAGAAGTCTCCAGAATCTCTGGTCAAGCTGGATGCAACCCCATTGTCC
TCCCCACGGCATGTGAGGATCAAAAACTGGGGCAGCGGGATGACTTTCCAAG
ACACACTTCACCATAAGGCCAAAGGGATTTTAACTTGCAGGTCCAAATCTTG
CCTGGGGTCCATTATGACTCCCAAAAGTTTGACCAGAGGACCCAGGGACAAG
CCTACCCCTCCAGATGAGCTTCTACCTCAAGCTATCGAATTTGTCAACCAATA
TTACGGCTCCTTCAAAGAGGCAAAAATAGAGGAACATCTGGCCAGGGTGGA
AGCGGTAACAAAGGAGATAGAAACAACAGGAACCTACCAACTGACGGGAGA
TGAGCTCATCTTCGCCACCAAGCAGGCCTGGCGCAATGCCCCACGCTGCATT
GGGAGGATCCAGTGGTCCAACCTGCAGGTCTTCGATGCCCGCAGCTGTTCCA
CTGCCCGGGAAATGTTTGAACACATCTGCAGACACGTGCGTTACTCCACCAA
CAATGGCAACATCAGGTCGGCCATCACCGTGTTCCCCCAGCGGAGTGATGGC
AAGCACGACTTCCGGGTGTGGAATGCTCAGCTCATCCGCTATGCTGGCTACC
AGATGCCAGATGGCAGCATCAGAGGGGACCCTGCCAACGTGGAATTCACTCA
GCTGTGCATCGACCTGGGCTGGAAGCCCAAGTACGGCCGCTTCGATGTGGTC
CCCCTGGTCCTGCAGGCCAATGGCCGTGACCCTGAGCTCTTCGAAATCCCACC
TGACCTTGTGCTTGAGGTGGCCATGGAACATCCCAAATACGAGTGGTTTCGG
GAACTGGAGCTAAAGTGGTACGCCCTGCCTGCAGTGGCCAACATGCTGCTTG
AGGTGGGCGGCCTGGAGTTCCCAGGGTGCCCCTTCAATGGCTGGTACATGGG
CACAGAGATCGGAGTCCGGGACTTCTGTGACGTCCAGCGCTACAACATCCTG
GAGGAAGTGGGCAGGAGAATGGGCCTGGAAACGCACAAGCTGGCCTCGCTC
TGGAAAGACCAGGCTGTCGTTGAGATCAACATTGCTGTGCTCCATAGTTTCCA
GAAGCAGAATGTGACCATCATGGACCACCACTCGGCTGCAGAATCCTTCATG
AAGTACATGCAGAATGAATACCGGTCCCGTGGGGGCTGCCCGGCAGACTGGA
TTTGGCTGGTCCCTCCCATGTCTGGGAGCATCACCCCCGTGTTTCACCAGGAG
ATGCTGAACTACGTCCTGTCCCCTTTCTACTACTATCAGGTAGAGGCCTGGAA
AACCCATGTCTGGCAGGACGAGCCCACGAAGCGGCGAGCTATCGGCTTTAAG
AAATTGGCAGAGGCCGTCAAGTTCTCAGCCAAGCTAATGGGGCAGGCCATGG
CCAAGAGGGTCAAGGCGACCATTCTCTACGCCACAGAGACAGGCAAATCAC
AAGCCTATGCCAAGACCCTGTGTGAGATCTTCAAGCACGCCTTCGATGCCAA
GGCAATGTCCATGGAGGAGTATGACATCGTGCACCTGGAGCACGAAGCCCTG
GTCTTGGTGGTCACCAGCACCTTTGGCAATGGAGACCCCCCTGAGAACGGGG
AGAAATTCGGCTGTGCTTTAATGGAGATGAGGCACCCCAACTCTGTGCAGGA
GGAGAGAAAGAGCTACAAGGTCCGATTCAACAGCGTCTCCTCCTATTCTGAC
TCCCGAAAGTCATCGGGCGACGGACCCGACCTCAGAGACAACTTTGAAAGTA
CTGGACCCCTGGCCAATGTGAGGTTCTCAGTGTTCGGCCTCGGCTCTCGGGCG
TACCCCCACTTCTGTGCCTTTGGGCATGCGGTGGACACCCTCCTGGAGGAACT
GGGAGGGGAGAGGATTCTGAAGATGAGGGAGGGGGATGAGCTTTGCGGACA
GGAAGAAGCTTTCAGGACCTGGGCCAAGAAAGTCTTCAAGGCAGCCTGTGAT
GTGTTCTGCGTGGGGGATGACGTCAACATCGAGAAGGCGAACAACTCCCTCA
TTAGCAATGACCGAAGCTGGAAGAGGAACAAGTTCCGCCTCACGTATGTGGC
GGAAGCTCCAGATCTGACCCAAGGTCTTTCCAATGTTCACAAAAAACGAGTC
TCGGCTGCTCGACTCCTCAGCCGCCAAAACCTGCAAAGCCCTAAGTCCAGCC
GATCGACCATCTTCGTGCGTCTCCACACCAACGGGAATCAGGAGCTGCAGTA

CCAGCCAGGGGACCACCTGGGTGTCTTCCCCGGCAACCACGAGGACCTCGTG
AATGCACTCATTGAACGGCTGGAGGATGCACCGCCTGCCAACCACGTGGTGA
AGGTGGAGATGCTGGAGGAGAGGAACACTGCTCTGGGTGTCATCAGTAATTG
GAAGGATGAATCTCGCCTCCCACCCTGCACCATCTTCCAGGCCTTCAAGTACT
ACCTGGACATCACCACGCCGCCCACGCCCCTGCAGCTGCAGCAGTTCGCCTC
TCTGGCCACTAATGAGAAAGAGAAGCAGCGGTTGCTGGTCCTCAGCAAGGGG
CTCCAGGAATATGAGGAGTGGAAGTGGGGCAAGAACCCCACAATGGTGGAG
GTGCTGGAGGAGTTCCCGTCCATCCAGATGCCGGCTACACTTCTCCTCACTCA
GCTGTCGCTGCTGCAGCCTCGCTACTACTCCATCAGCTCCTCTCCAGACATGT
ACCCCGACGAGGTGCACCTCACTGTGGCCATCGTCTCCTACCACACCCGAGA
CGGAGAAGGACCAGTCCACCACGGGGTGTGCTCCTCCTGGCTCAACAGAATA
CAGGCTGACGATGTAGTCCCCTGCTTCGTGAGAGGTGCCCCTAGCTTCCACCT
GCCTCGAAACCCCCAGGTGCCTTGCATCCTGGTTGGCCCAGGCACTGGCATC
GCACCCTTCCGAAGCTTCTGGCAACAGCGACAATTTGACATCCAACACAAAG
GAATGAATCCGTGCCCCATGGTTCTGGTCTTCGGGTGTCGACAATCCAAGAT
AGATCATATCTACAGAGAGGAGACCCTGCAGGCCAAGAACAAGGGCGTCTTC
AGAGAGCTGTACACTGCCTATTCCCGGGAACCGGACAGGCCAAAGAAATATG
TACAGGACGTGCTGCAGGAACAGCTGGCTGAGTCTGTGTACCGCGCCCTGAA
GGAGCAAGGAGGCCACATTTATGTCTGTGGGGACGTTACCATGGCCGCCGAT
GTCCTCAAAGCCATCCAGCGCATAATGACCCAGCAGGGGAAACTCTCAGAGG
AGGACGCTGGTGTATTCATCAGCAGGCTGAGGGATGACAACCGGTACCACGA
GGACATCTTTGGAGTCACCCTCAGAACGTATGAAGTGACCAACCGCCTTAGA
TCTGAGTCCATCGCCTTCATCGAAGAGAGCAAAAAAGACGCAGATGAGGTTT
TCAGCTCCTAA

vi) coding sequence of NOSTIC-3 with N-terminal His6 tag and C-terminal FLAG tag:
ATGCATCATCACCATCACCATATGGCTTGTCCTTGGAAATTTCTGTTCAAGAC
CAAATTCCACCAGTATGCAATGAATGGGGAAAAAGACATCAACAACAATGT
GGAGAAAGCCCCCTGTGCCACCTCCAGTCCAGTGACACAGGATGACCTTCAG
TATCACAACCTCAGCAAGCAGCAGAATGAGTCCCCGCAGCCCCTCGTGGAGA
CGGGAAAGAAGTCTCCAGAATCTCTGGTCAAGCTGGATGCAACCCCATTGTC
CTCCCCACGGCATGTGAGGATCAAAAACTGGGGCAGCGGGATGACTTTCCAA
GACACACTTCACCATAAGGCCAAAGGGATTTTAACTTGCAGGTCCAAATCTT
GCCTGGGGTCCATTATGTTCCCCAAAAGTTTGACCAGAGGACCCAGGGACAA
GCCTACCCCTCCAGATGAGCTTCTACCTCAAGCTATCGAATTTGTCAACCAAT
ATTACGGCTCCTTCAAAGAGGCAAAAATAGAGGAACATCTGGCCAGGGTGG
AAGCGGTAACAAAGGAGATAGAAACAACAGGAACCTACCAACTGACGGGAG
ATGAGCTCATCTTCGCCACCAAGCAGGCCTGGCGCAATGCCCCACGCTGCAT
TGGGAGGATCCAGTGGTCCAACCTGCAGGTCTTCGATGCCCGCAGCTGTTCC
ACTGCCCGGGAAATGTTTGAACACATCTGCAGACACGTGCGTTACTCCACCA
ACAATGGCAACATCAGGTCGGCCATCACCGTGTTCCCCCAGCGGAGTGATGG
CAAGCACGACTTCCGGGTGTGGAATGCTCAGCTCATCAAGTATGCTGGCTAC
CAGATGCCAGATGGCAGCATCAGAGGGGACCCTGCCAACGTGGAATTCACTC
AGCTGTGCATCGACCTGGGCTGGAAGCCCAAGTACGGCCGCTTCGATGTGGT
CCCCCTGGTCCTGCAGGCCAATGGCCGTGACCCTGAGCTCTTCGAAATCCCAC
CTGACCTTGTGCTTGAGGTGGCCATGGAACATCCCAAATACGAGTGGTTTCG

GGAACTGGAGCTAAAGTGGTACGCCCTGCCTGCAGTGGCCAACATGCTGCTT
GAGGTGGGCGGCCTGGAGTTCCCAGGGTGCCCCTTCAATGGCTGGTACATGG
GCACAGAGATCGGAGTCCGGGACTTCTGTGACGTCCAGCGCTACAACATCCT
GGAGGAAGTGGGCAGGAGAATGGGCCTGGAAACGCACAAGCTGGCCTCGCT
CTGGAAAGACCAGGCTGTCGTTGAGATCAACATTGCTGTGCTCCATAGTTTCC
AGAAGCAGAATGTGACCATCATGGACCACCACTCGGCTGCAGAATCCTTCAT
GAAGTACATGCAGAATGAATACCGGTCCCGTGGGGGCTGCCCGGCAGACTGG
ATTTGGCTGGTCCCTCCCATGTCTGGGAGCATCACCCCCGTGTTTCACCAGGA
GATGCTGAACTACGTCCTGTCCCCTTTCTACTACTATCAGGTAGAGGCCTGGA
AAACCCATGTCTGGCAGGACGAGCCCACGAAGCGGCGAGCTATCGGCTTTAA
GAAATTGGCAGAGGCCGTCAAGTTCTCAGCCAAGCTAATGGGGCAGGCCATG
GCCAAGAGGGTCAAGGCGACCATTCTCTACGCCACAGAGACAGGCAAATCA
CAAGCCTATGCCAAGACCCTGTGTGAGATCTTCAAGCACGCCTTCGATGCCA
AGGCAATGTCCATGGAGGAGTATGACATCGTGCACCTGGAGCACGAAGCCCT
GGTCTTGGTGGTCACCAGCACCTTTGGCAATGGAGACCCCCCTGAGAACGGG
GAGAAATTCGGCTGTGCTTTAATGGAGATGAGGCACCCCAACTCTGTGCAGG
AGGAGAGAAAGAGCTACAAGGTCCGATTCAACAGCGTCTCCTCCTATTCTGA
CTCCCGAAAGTCATCGGGCGACGGACCCGACCTCAGAGACAACTTTGAAAGT
ACTGGACCCCTGGCCAATGTGAGGTTCTCAGTGTTCGGCCTCGGCTCTCGGGC
GTACCCCCACTTCTGTGCCTTTGGGCATGCGGTGGACACCCTCCTGGAGGAAC
TGGGAGGGGAGAGGATTCTGAAGATGAGGGAGGGGGATGAGCTTTGCGGAC
AGGAAGAAGCTTTCAGGACCTGGGCCAAGAAAGTCTTCAAGGCAGCCTGTGA
TGTGTTCTGCGTGGGGGATGACGTCAACATCGAGAAGGCGAACAACTCCCTC
ATTAGCAATGACCGAAGCTGGAAGAGGAACAAGTTCCGCCTCACGTATGTGG
CGGAAGCTCCAGATCTGACCCAAGGTCTTTCCAATGTTCACAAAAAACGAGT
CTCGGCTGCTCGACTCCTCAGCCGCCAAAACCTGCAAAGCCCTAAGTCCAGC
CGATCGACCATCTTCGTGCGTCTCCACACCAACGGGAATCAGGAGCTGCAGT
ACCAGCCAGGGGACCACCTGGGTGTCTTCCCCGGCAACCACGAGGACCTCGT
GAATGCACTCATTGAACGGCTGGAGGATGCACCGCCTGCCAACCACGTGGTG
AAGGTGGAGATGCTGGAGGAGAGGAACACTGCTCTGGGTGTCATCAGTAATT
GGAAGGATGAATCTCGCCTCCCACCCTGCACCATCTTCCAGGCCTTCAAGTAC
TACCTGGACATCACCACGCCGCCCACGCCCCTGCAGCTGCAGCAGTTCGCCT
CTCTGGCCACTAATGAGAAAGAGAAGCAGCGGTTGCTGGTCCTCAGCAAGGG
GCTCCAGGAATATGAGGAGTGGAAGTGGGGCAAGAACCCCACAATGGTGGA
GGTGCTGGAGGAGTTCCCGTCCATCCAGATGCCGGCTACACTTCTCCTCACTC
AGCTGTCGCTGCTGCAGCCTCGCTACTACTCCATCAGCTCCTCTCCAGACATG
TACCCCGACGAGGTGCACCTCACTGTGGCCATCGTCTCCTACCACACCCGAG
ACGGAGAAGGACCAGTCCACCACGGGGTGTGCTCCTCCTGGCTCAACAGAAT
ACAGGCTGACGATGTAGTCCCCTGCTTCGTGAGAGGTGCCCCTAGCTTCCACC
TGCCTCGAAACCCCCAGGTGCCTTGCATCCTGGTTGGCCCAGGCACTGGCATC
GCACCCTTCCGAAGCTTCTGGCAACAGCGACAATTTGACATCCAACACAAAG
GAATGAATCCGTGCCCCATGGTTCTGGTCTTCGGGTGTCGACAATCCAAGAT
AGATCATATCTACAGAGAGGAGACCCTGCAGGCCAAGAACAAGGGCGTCTTC
AGAGAGCTGTACACTGCCTATTCCCGGGAACCGGACAGGCCAAAGAAATATG
TACAGGACGTGCTGCAGGAACAGCTGGCTGAGTCTGTGTACCGCGCCCTGAA
GGAGCAAGGAGGCCACATTTATGTCTGTGGGGACGTTACCATGGCCGCCGAT

GTCCTCAAAGCCATCCAGCGCATAATGACCCAGCAGGGGAAACTCTCAGAGG
AGGACGCTGGTGTATTCATCAGCAGGCTGAGGGATGACAACCGGTACCACGA
GGACATCTTTGGAGTCACCCTCAGAACGTATGAAGTGACCAACCGCCTTAGA
TCTGAGTCCATCGCCTTCATCGAAGAGAGCAAAAAAGACGCAGATGAGGTTT
TCAGCTCCGGATCTGATTACAAAGACGACGACGACAAGTAA

vii) coding sequence of α_1AR with C-terminal V5 tag:
ATGGTGTTTCTCTCGGGAAATGCTTCCGACAGCTCCAACTGCACCCAACCGCC
GGCACCGGTGAACATTTCCAAGGCCATTCTGCTCGGGGTGATCTTGGGGGGC
CTCATTCTTTTCGGGGTGCTGGGTAACATCCTAGTGATCCTCTCCGTAGCCTG
TCACCGACACCTGCACTCAGTCACGCACTACTACATCGTCAACCTGGCGGTG
GCCGACCTCCTGCTCACCTCCACGGTGCTGCCCTTCTCCGCCATCTTCGAGGT
CCTAGGCTACTGGGCCTTCGGCAGGGTCTTCTGCAACATCTGGGCGGCAGTG
GATGTGCTGTGCTGCACCGCGTCCATCATGGGCCTCTGCATCATCTCCATCGA
CCGCTACATCGGCGTGAGCTACCCGCTGCGCTACCCAACCATCGTCACCCAG
AGGAGGGGTCTCATGGCTCTGCTCTGCGTCTGGGCACTCTCCCTGGTCATATC
CATTGGACCCCTGTTCGGCTGGAGGCAGCCGGCCCCCGAGGACGAGACCATC
TGCCAGATCAACGAGGAGCCGGGCTACGTGCTCTTCTCAGCGCTGGGCTCCT
TCTACCTGCCTCTGGCCATCATCCTGGTCATGTACTGCCGCGTCTACGTGGTG
GCCAAGAGGGAGAGCCGGGGCCTCAAGTCTGGCCTCAAGACCGACAAGTCG
GACTCGGAGCAAGTGACGCTCCGCATCCATCGGAAAAACGCCCCGGCAGGA
GGCAGCGGGATGGCCAGCGCCAAGACCAAGACGCACTTCTCAGTGAGGCTCC
TCAAGTTCTCCCGGGAGAAGAAAGCGGCCAAAACGCTGGGCATCGTGGTCGG
CTGCTTCGTCCTCTGCTGGCTGCCTTTTTTCTTAGTCATGCCCATTGGGTCTTT
CTTCCCTGATTTCAAGCCCTCTGAAACAGTTTTTAAAATAGTATTTTGGCTCG
GATATCTAAACAGCTGCATCAACCCCATCATATACCCATGCTCCAGCCAAGA
GTTCAAAAAGGCCTTTCAGAATGTCTTGAGAATCCAGTGTCTCTGCAGAAAG
CAGTCTTCCAAACATGCCCTGGGCTACACCCTGCACCCGCCCAGCCAGGCCG
TGGAAGGGCAACACAAGGACATGGTGCGCATCCCCGTGGGATCAAGAGAGA
CCTTCTACAGGATCTCCAAGACGGATGGCGTTTGTGAATGGAAATTTTTCTCT
TCCATGCCCCGTGGATCTGCCAGGATTACAGTGTCCAAAGACCAATCCTCCTG
TACCACAGCCCGGGTGAGAAGTAAAAGCTTTTTGCAGGTCTGCTGCTGTGTA
GGGCCCTCAACCCCCAGCCTTGACAAGAACCATCAAGTTCCAACCATTAAGG
TCCACACCATCTCCCTCAGTGAGAACGGGGAGGAAGTCGGTAAACCTATTCC
TAACCCACTTCTGGGTCTCGATAGCACATAG

viii) Hippo-HFt
ATGGGCAAGCAGAATAGCAAGCTGCGGCCAGAGATGCTGCAGGACCTGCGA
GAGAACACCGAGTTCTCTGAGCTGGAGCTTCAGGAGTGGTACAAGGGCTTCC
TGAAGGACTGCCCGACTGGCATCCTCAACGTGGATGAGTTCAAGAAGATCTA
CGCCAACTTCTTCCCCTACGGCGATGCCTCCAAGTTCGCCGAGCATGTCTTCC
GCACTTTTGACACCAACAGCGACGGCACCATCGACTTCCGGGAGTTCATCAT
CGCTCTGAGCGTGACCTCGCGTGGCCGCCTGGAGCAGAAGCTCATGTGGGCC
TTCAGCATGTACGACCTGGACGGCAATGGCTACATCAGCCGGGAGGAGATGC
TAGAAATTGTGCAGGCCATTTACAAGATGGTTTCGTCCGTGATGAAGATGCC
TGAGGATGAGTCTACCCCGGAAAAGAGGACTGAGAAAATCTTCCGCCAAATG

GACACAAACAATGACGGCAAGCTGTCACTGGAGGAATTCATCCGCGGGGCC
AAAAGCGACCCATCGATCGTGCGCCTGCTGCAATGCGATCCCAGCAGCGCTT
CCCAGTTCTCGGCCAGCGGAGCCGGTGGATGGAGCCACCCGCAGTTCGAGAA
AGGAACATCTGGGGCTACAACGACCGCGTCCACCTCGCAGGTGCGCCAGAAC
TACCACCAGGACTCAGAGGCCGCCATCAACCGCCAGATCAACCTGGAGCTCT
ACGCCTCCTACGTTTACCTGTCCATGTCTTACTACTTTGACCGCGATGATGTG
GCCTTGAAGAACTTTGCCAAATACTTTCTTCACCAATCTCATGAGGAGAGGG
AACATGCTGAGAAACTGATGAAGCTGCAGAACCAACGAGGTGGCCGAATCTT
CCTTCAGGATATCAAGAAACCAGACTGTGATGACTGGGAGAGCGGGCTGAAT
GCGATGGAGTGTGCATTACATTTGGAAAAAAATGTGAATCAGTCACTACTGG
AACTGCACAAACTGGCCACTGACAAAAATGACCCCCATTTGTGTGACTTCAT
TGAGACACATTACCTGAATGAGCAGGTGAAAGCCATCAAAGAATTGGGTGAC
CACGTGACCAACTTGCGCAAGATGGGAGCGCCCGAATCCGGCTTGGCGGAAT
ATCTCTTTGACAAGCACACCCTGGGAGACAGTGATAATGAAAGCTAA

ix) Hippo-EcFtnA
ATGGGCAAGCAGAATAGCAAGCTGCGGCCAGAGATGCTGCAGGACCTGCGA
GAGAACACCGAGTTCTCTGAGCTGGAGCTTCAGGAGTGGTACAAGGGCTTCC
TGAAGGACTGCCCGACTGGCATCCTCAACGTGGATGAGTTCAAGAAGATCTA
CGCCAACTTCTTCCCCTACGGCGATGCCTCCAAGTTCGCCGAGCATGTCTTCC
GCACTTTTGACACCAACAGCGACGGCACCATCGACTTCCGGGAGTTCATCAT
CGCTCTGAGCGTGACCTCGCGTGGCCGCCTGGAGCAGAAGCTCATGTGGGCC
TTCAGCATGTACGACCTGGACGGCAATGGCTACATCAGCCGGGAGGAGATGC
TAGAAATTGTGCAGGCCATTTACAAGATGGTTTCGTCCGTGATGAAGATGCC
TGAGGATGAGTCTACCCCGGAAAAGAGGACTGAGAAAATCTTCCGCCAAATG
GACACAAACAATGACGGCAAGCTGTCACTGGAGGAATTCATCCGCGGGGCC
AAAAGCGACCCATCGATCGTGCGCCTGCTGCAATGCGATCCCAGCAGCGCTT
CCCAGTTCTCGGCCAGCGGAGCCGGTGGATGGAGCCACCCGCAGTTCGAGAA
AGGAACATCTGGGGCTACAATGCTGAAACCAGAAATGATTGAAAAACTTAAT
GAGCAGATGAACCTGGAACTGTACTCTTCACTGCTTTATCAGCAAATGAGCG
CCTGGTGCAGCTATCATACCTTCGAAGGTGCTGCCGCGTTCCTGCGCCGTCAC
GCCCAGGAAGAGATGACGCATATGCAGCGTCTGTTTGATTACCTGACTGATA
CCGGCAATTTACCGCGTATTAATACCGTTGAATCTCCGTTTGCTGAATATTCC
TCACTTGATGAATTATTCCAGGAAACCTATAAACACGAACAATTAATCACCC
AGAAAATTAACGAACTGGCTCATGCTGCAATGACCAATCAGGACTACCCAAC
ATTTAATTTCCTGCAATGGTATGTTTCTGAGCAGCATGAAGAAGAGAAACTG
TTCAAATCGATTATTGATAAATTAAGCCTGGCAGGCAAAAGCGGCGAAGGTC
TGTATTTTATCGACAAAGAACTCTCTACCCTCGACACACAAAACTAA

x) Hippo-AA
ATGGGCAAGCAGAATAGCAAGCTGCGGCCAGAGATGCTGCAGGACCTGCGA
GAGAACACCGAGTTCTCTGAGCTGGAGCTTCAGGAGTGGTACAAGGGCTTCC
TGAAGGACTGCCCGACTGGCATCCTCAACGTGGATGAGTTCAAGAAGATCTA
CGCCAACTTCTTCCCCTACGGCGATGCCTCCAAGTTCGCCGAGCATGTCTTCC
GCACTTTTGACACCAACAGCGACGGCACCATCGACTTCCGGGAGTTCATCAT
CGCTCTGAGCGTGACCTCGCGTGGCCGCCTGGAGCAGAAGCTCATGTGGGCC

TTCAGCATGTACGACCTGGACGGCAATGGCTACATCAGCCGGGAGGAGATGC
TAGAAATTGTGCAGGCCATTTACAAGATGGTTTCGTCCGTGATGAAGATGCC
TGAGGATGAGTCTACCCCGGAAAAGAGGACTGAGAAAATCTTCCGCCAAATG
GACACAAACAATGACGGCAAGCTGTCACTGGAGGAATTCATCCGCGGGGCC
AAAAGCGACCCATCGATCGTGCGCCTGCTGCAATGCGATCCCAGCAGCGCTT
CCCAGTTCTCGGCCAGCGGAGCCGGTGGAAGCGAAGGTGGAGGAAGCGAGG
GCGGAACATCTGGGGCTACAATGGCATCCATTTCTGAAAAAATGGTTGAGGC
TTTGAACAGGCAGATAAACGCTGAAATCTACTCAGCATACCTCTACCTCTCCA
TGGCCTCTTACTTCGACTCCATCGGGCTTAAGGGCTTCTCAAACTGGATGAGG
GTGCAGTGGCAGGAGGAGCTGATGCATGCGATGAAGATGTTTGACTTTGTCA
GTGAGAGGGGAGGGAGAGTTAAGCTCTACGCTGTTGAGGAGCCACCATCTGA
GTGGGATTCGCCTTTGGCAGCCTTTGAGCACGTTTACGAGCATGAGGTAAAT
GTTACGAAGAGAATTCACGAGCTTGTTGAGATGGCAATGCAGGAAAAGGACT
TTGCAACCTACAACTTCCTGCAGTGGTATGTTGCGGAGCAGGTTGAGGAGGA
AGCCTCTGCCCTCGACATTGTGGAGAAGCTGAGGTTGATTGGAGAGGACGCA
GCAGCTTTGCTTTTCCTTGATAAGGAGCTTTCTCTCAGGCAGTTTACTCCTCCA
GCTGAGGAGGAGAAGTAA